SSRG International Journal of Thermal Engineering
ISSN: 2395-0250/ https://doi.org/10.14445/23950250/IJTE-V12I1P101

Volume 12 Issue 1, 1-26, Jan-Apr 2026
© 2026 Seventh Sense Research Group®

Original Article

A Novel Concept of Solar Photovoltaic-Thermal, Heat Pipe, and Heat Pump Hybrid

S. Sami[1,2]

[1]*TransPacific Energy, Inc., NV, USA.*
[2]*Mechanical Engineering, UNLV, Las Vegas, NV, USA.*

[1]*Corresponding Author : dr.ssamiu@transpacenergy.com*

Received: 01 December 2025 Revised: 02 January 2026 Accepted: 21 January 2026 Published: 07 February 2026

Abstract *- A numerical prediction of a Novel Hybrid System Concept, composed of Photovoltaic-Thermal Solar Panels and a Heat Pipe, is presented here. This model is presented to assess the performance and energy conversion process of the Hybrid System, as well as the individual efficiencies of this process to produce hot water and electricity. A Two-Dimensional Heat Transfer and Fluid Flow Dynamic Model was developed and presented to describe the behavior of a Hybrid System under various Solar Irradiance Conditions, Heat Pipe Configurations, and Different Refrigerants. The model is based upon Dynamic Mass and Energy Equations coupled with the Heat Transfer Formulas, and Thermodynamic Properties of Refrigerants, as well as Thermal Material Properties of the PV solar panel and heat pipes. Finally, the presented model has been validated, and its predictions are in fair agreement with available data.*

Keywords *- Numerical Modeling, Simulation, Photovoltaic-Thermal Solar, Heat Pipe, Refrigerants, Hybrid System Performance, Model Validation.*

1. Introduction

New PV technologies reported in the literature [1-34] have been shown to improve the energy utilization efficiency of solar PV, such as multi-junction cells, Optical Frequency Shifting, and Concentrated Photovoltaic (CPV) Systems, among others; however, they are expensive. Harvesting energy from the sun is a promising technology to resolve the ongoing energy crisis. Solar Photovoltaic (PV) and Photovoltaic/Thermal (PV/T) systems are mainstream solar energy conversion technologies that enable dual functions, providing both electrical and thermal energy.

Heat pipes are becoming increasingly popular as passive heat transfer technologies due to their high efficiency when the appropriate refrigerants are used. Heat pipes are currently utilized in widespread industrial applications, such as solar, nanoparticles, Rankine cycles, nuclear, thermoelectric modules, and ceramics, in which heat pipe technologies offer many key advantages over conventional practices, including nanofluids for higher thermal conductivity.

Phase Change Materials (PCM) integrated behind PV for thermal buffering, selective coatings optimized for combined PV/thermal absorption. The combination optimizes the use of solar energy, functioning as a heat source for water heating and mitigating the low PV efficiency issue caused by the module's high temperature.

Therefore, this research aimed to investigate and compare the efficiency of PV, PV/T, and PV/T with a Heat Pipe (HP). We provide a novel review of Solar PV-Thermal (PVT) systems, heat pipes, and heat pumps, with emphasis on what is genuinely new. The recent Key Novel Advances are summarized in spectral splitting PVT, Concentrated PVT (CPVT) with low-to-medium concentration: vacuum-insulated PVT to reduce convective losses, dual-fluid PVT. The research gap includes the long-term stability of nanofluids, PCM degradation under cyclic PV heat, and AI-Optimized PVT Systems.

Novelty in Nanofluid-based heat pipes, Low-GWP refrigerants and bio-fluids, Hybrid PCM–heat pipe structures. Primary Novel Directions in heat pumps: Solar-Coupled Heat Pumps, PVT as a low-temperature source for heat pumps, dynamic switching between PV-only, thermal-only, or hybrid modes. Novelty in heat pump developments is in ML-based demand forecasting, reinforcement learning for compressor and expansion valve control, and predictive defrosting algorithms. Unlike conventional PVT systems, this work integrates AI-driven control with heat pipe-enhanced thermal regulation and heat pump coupling. This study moves beyond component optimization to system-level intelligence and adaptability. The novelty lies in the co-optimization of electrical, thermal, and upgraded heat outputs under real-time environmental and demand uncertainty.

This is an open access article under the CC BY-NC-ND license (http://creativecommons.org/licenses/by-nc-nd/4.0/)

In order to improve the solar PV's efficiency, a novel concept of a combined Photovoltaic-Thermal Solar Panel Hybrid System has been developed and implemented [3-12], where the PV cells of the solar PV panels are cooled by water flows. Excess thermal energy is generated and dissipated due to the intrinsic conversion efficiency limitation of the cell. The dissipated and excess thermal energy increases the cell temperature and, in turn, reduces the conversion efficiency of the cell. The excess thermal energy absorbed by the cold-water flows through the heat exchanger thermal panel underneath the PV cell and can be used for various domestic or industrial applications. Therefore, the net result is an enhancement of the combined Photovoltaic-Thermal efficiency of the hybrid system.

Endalew [9] in his master's thesis studied the performance of Heat Pipe Solar collectors for water heating. Experimental results were validated using numerical modeling. Heat pipes with distilled water as the working fluid were used for experimental tests. Both natural and forced convective heat pipe condensing mechanisms were studied, and their results were compared with conventional natural circulation solar water heating systems. Crossflow and parallel flow heat exchangers were also tested in a forced-type heat pipe condensing mechanism. Experimental and numerical results showed good agreement. Heat pipe solar collectors outperformed conventional solar collectors because of their efficient heat transport method. The forced convective heat exchanger was found to give higher efficiency compared to the natural convective heat pipe condensing system.

A Hybrid Photovoltaic Solar-assisted loop heat pipe/heat pump (PV-SALHP/HP) water heater system has been developed and numerically studied by Dai et al. [3]. The system is the combination of Loop Heat Pipe (LHP) mode and Heat Pump (HP) Mode, and the two modes can be run separately or in combination according to the weather conditions. The performances of the independent Heat Pump (HP) Mode and Hybrid Loop Heat Pipe/Heat Pump (LHP/HP) mode were simulated and compared. Simulation results showed that on typical sunny days in spring or autumn, using LHP/HP mode could save 40.6% more power consumption than HP mode.

Heat pipes are effective and Passive Heat Transfer devices that are capable of transferring heat with a slight temperature differences between the heat source and the heat sink. A heat pipe is generally made of a sealed copper pipe, evacuated, and filled with working fluid such as a refrigerant that boils at low temperatures. The distinct sections of the heat pipes are the evaporator section, the condenser section, and the adiabatic section, where no heat transfer between the refrigerant and the heat source or heat sink occurs. Heat absorbed at the evaporator section of the pipe boils the working fluid inside the heat pipe and vaporizes it with the latent heat of vaporization. This vapor of the working fluid inside the heat pipe is condensed in the condenser section, where it releases its latent heat of condensation. The condensate working fluid is then channeled back to the evaporator section due to gravity and internal wicks. Readers interested in the comprehensive discussions of the heat pipes' heat transfer mechanisms are advised to consult references [1-3, 20, 24-28].

A Novel Heat-Pipe Photovoltaic/Thermal System was designed and constructed by Pei et al. [2] to supply simultaneously Electrical and Thermal Energy. The authors developed a dynamic model to predict the performance of the Heat-Pipe Photovoltaic/Thermal System. Experiments were also conducted to validate the numerical results obtained during the simulation. A comparison between simulation values and experimental results demonstrated that the model was able to yield satisfactory predictions.

Another transient mathematical model for the integrated HP-PV/T-PCM system presented by Sweidan et al. [26] was used to predict its performance under solar conditions and PCM melting point. The model was validated and applied to a typical office space in the city of Beirut to obtain an optimal design using a derivative-free genetic algorithm. The incremental system cost associated with a heat pipe and PCM tank was used in the optimization to obtain a design resulting in a minimum annual auxiliary heating cost to meet the hot water demand while providing the electricity needs at a lower number of PV panels due to improved efficiency.

On the other hand, Liang et al. [12] presented a Dynamic Model of a novel solar heating system based on Hybrid Photovoltaic/Thermal and Heat Pipes Technology. The TRNSYS simulation platform of the PVT cogeneration heating system has been implemented for predicting the system performance of the PVT solar cogeneration heating system. The inlet and outlet temperature, the electrical power output of the PVT collector, heat consumption, outlet temperatures of the auxiliary heat source, and outlet temperatures of the heat storage tank of the PVT collector have been studied in this paper. The results of this investigation showed heat gain of the heat collector system between 12 am and 6 pm on a typical day, 'when the auxiliary heat source is not turned on and can meet the load demand. During the entire heating season, the solar fraction of this solar heating system is 31.7%, which is close to the design value of 30%.

The model introduced by Naghavi [29] is the integration of a Heat Pipe Solar Water Heater System (HPSWH) with Phase Change Material (PCM) to control the overheating of supplied water during the day and extend the operation time of the solar water heater system. The heat pipe needs to be adjusted concerning the amount of absorbed Solar Radiation Energy. On the other hand, PCM is placed at the bottom of

the solar absorber plate and heat pipe to absorb and store extra thermal energy gained by the absorber plate, which is not collected by the heat pipe. Approximate analytical solutions have been used to estimate the amount of absorbed solar energy and the thermal behavior of supplying water. A one-phase approximation solution is applied to estimate the thickness and stored energy of PCM. The results of this research indicate the feasibility of integrating PCM to improve the overall performance of the HPSWH system.

Future directions for Solar PV-Thermal (PVT) systems involve: Solar PV-Thermal (PVT) Systems, AI-driven intelligent control & optimization, spectral & optical design innovations, high-temperature PVT & Storage integration, and lifecycle, degradation & reliability studies. On the other hand, future trends in heat pipes and two-phase thermal management include innovative/adaptive heat pipes, integrated heat pipes in solar and thermal systems, novel working fluids and wick structures, and additive manufacturing for custom heat pipe topologies. To this end, heat pumps (especially Solar-Integrated) can involve Solar-Assisted & PVT-Coupled Heat Pumps, AI and predictive Heat Pump Control, new refrigerants & cycle architectures, and non-HVAC applications.

The modeling and simulation of a Novel Hybrid System of Solar Photovoltaic-Thermal Panels and Heat Pipes is presented in this paper. A schematic diagram of the thermal Solar-Heat Pipes Hybrid System under study is shown in Figure 1. This novel concept is intended to enhance the energy conversion efficiency of the PV-Thermal solar/heat pipe hybrid system by recovering the excess thermal energy dissipated by the energy conversion process of the solar PV panels to produce Domestic Hot Water (DHW). This consequently enhances the energy conversion efficiency of the Solar Photovoltaic and the Hybrid System. The conceptual Photovoltaic-Thermal Panel integrated heat pipes design was modeled and analyzed using a two-dimensional dynamic model based on the heat transfer and fluid flow conversion equations. The model was developed to describe the steady state and dynamic thermal behavior of a combined photovoltaic cell-thermal panel as well as the heat pipes hybrid system under different solar irradiances, material properties, ambient and fluid flow conditions, refrigerants contained in the heat pipes, and excess thermal energy recovered by the panel, as well as boundary conditions. The predicted results presented herein include the efficiency of the energy conversion process of the Hybrid System, PV cell characteristics, and heat pipes' behavior with different refrigerants, and finally, the thermal energy recovered by the hybrid system panel and delivered for domestic and/or industrial use under different conditions.

1.1. Mathematical Model

The study presented herein is based partly on the concept reported by Yang et al. [1] and an extension of the modeling reported by Sami and Campoverde [27], where a flat plate solar collector is attached to a PV panel. The Hybrid System in question is composed of the PV Solar Panel and Thermal Solar Tube Collector, as well as the heat pipe and thermal tank, as shown in Figure 1. This Hybrid System consists of a Photovoltaic Panel welded on the backside and thin parallel tubes for the circulation of the cooling fluid. The various flow tubes in contact with the PV solar panel are connected to a heat exchanger, where the evaporator section of the heat pipe is placed. The water flows through the thermal solar collector copper pipes and carries the recovered excess heat away from the solar PV panel and thermal panel, as shown in Figure 1. The heat pipe condenser section is placed in a thermal tank, supplying the demand for hot water.

A typical PV panel output is in DC and connected to a load controller and batteries, as well as an inverter for converting the DC output into AC for potential use in applications where AC is required. In the following sections, the energy conversion process and the enhancement of the Hybrid System efficiency, as well as the characteristics of Solar PV/Thermal Panels, and Heat Pipes, are presented at various operating temperatures, different solar radiation, and different refrigerants filled in the Heat Pipe.

1.2. Solar PV MODEL

The Solar Photovoltaic Panel is constructed of various modules, and each module consists of arrays and cells. The dynamic current output can be obtained as follows [13-15], [17], and [27,28].

$$I_P = I_L - I_o \left[exp\left(\frac{q(V+I_P R_S)}{AkT_C} - \frac{V+I_P R_S}{R_{sh}} \right) \right] \quad (1)$$

I_p: Output current of the PV module
I_L: Light-generated current per module
I_o: Reverse saturation current per module
V: Terminal voltage per module
R_s: Diode series resistance per module
R_{sh}: Diode shunt resistance per module
q: Electric charge
k: The Boltzmann constant
A: Diode ideality factor for the module

Were.

$$I_o = BT^3 c \left[exp\left(-\frac{E_{go}}{KT_C} \right) \right] \quad (2)$$

And.

$$I_L = P_1 G[1 - P_2(G - G_r) + P_3(T_C - T_r)] \quad (3)$$

Were.

The PV cell temperature, Tc, is influenced by various factors such as solar radiation, ambient conditions, and wind speed. It is well known that the cell temperature impacts the PV output current and performance, and its time variation can be determined from references [2, 19-22]. The AC power of the inverter output P(t) is calculated using the inverter

efficiency. η_{inv} , output voltage between phases, neutral V_{fn}, and for single-phase current I_o And $cos\varphi$ As follows.

$$P(t) = \sqrt{3}\eta_{inv}V_{fn}I_o cos\varphi \quad (4)$$

1.3. PV Thermal Model

The following thermal analysis is performed for a single PV cell; however, it is assumed that all PV cells behave the same, therefore, it can be applied to the whole PV solar panel.

The heat absorbed by the PV solar cell can be calculated as follows [27].

$$Q_{in} = \alpha_{abs} G S_p \quad (5)$$

Were.
α_{abs}: Overall absorption coefficient
G: Total Solar radiation incident on the PV module
S_p: Total area of the PV module

Meanwhile, the PV cell Temperature is computed from the following heat balance [27,28].

$$mC_{p\_module}\frac{dT_C}{dt} = Q_{in} - Q_{conv} - Q_{elect} \quad (6)$$

Were.
T_C: PV Cell Temperature
mC_{p_module}: Thermal capacity of the PV module
t: time
Q_{in}: Energy received due to solar irradiation, equation (4)
Q_{conv}: Energy loss due to Convection
Q_{elect}: Electrical power generated

1.4. Thermal energy incident on a PV cell

The thermal energy transferred from the PV cell to the Heat Transfer Fluid (HTF) is determined from the heat balance across the PV cell and HTF in terms of the heat transfer mechanisms: conduction, Convection, and radiation, as follows [27,28].

The heat transfer by conduction is.

$$Q_{conduction} = \frac{K_{Pv} \times \Delta T(T_c - T_m)}{L_{cell}} \quad (7)$$

T_m: Module Back-surface temperature
K_{Pv}: Thermal conductivity of PV cell
L_{cell}: Length of a PV cell

The heat transfer by Convection is determined from.

$$Q_{convection} = h_{water} \times \Delta T(T_m - T_f) \quad (8)$$

$Q_{convection}$: Energy due to Convection
h_{water}: Heat transfer coefficient
T_f: Fluid temperature

The heat transfer by radiation is.

$$Q_{radiation} = \varepsilon \times \sigma(T_m^{\,4} - T_f^{\,4}) \quad (9)$$

$Q_{convection}$: Energy due to radiation
ε:Emissivity PV cell
σ: Stefan-Boltzmann constant

The finite difference formulation is used to determine the heat transfer fluid temperatures at each element, where each heat transfer fluid tube is divided into several thermal elements.

$$T_f = T_{f\_in} + \frac{\partial Q}{m_{water} C_p} \times t \quad (10)$$

$\dot{m}_w$: Water mass flow (HTF)
C_p: Specific heat of water.
t: time
δQ: the heat transfer per element
T_{f_in}: Fluid temperature at inlet

The thermal energy transferred from the back of the PV cell to the Heat Transfer Fluid (HTF) is obtained by.

$$Q_{Thermal} = \dot{m} \times C_{p\_water} \times \Delta T(T_{fHx+1} - T_{f\_In}) \quad (11)$$

Were.
$Q_{Thermal}$: Energy from the thermal process
T_{fHx+1}: Fluid temperature at thermal element (f+1)
$T_{f\text{-}in}$: Fluid temperature at thermal element (1)

The total energy transferred to the heat transfer fluid is calculated from the integration of equations (6) through (11) written for each element, dx, along the length of each tube.

It is worthwhile mentioning that the PV cell and panel temperature is influenced by different factors, in particular the ambient conditions such as the temperature, humidity, and wind speed, among other parameters.

The back-temperature T_m of the PV cell and PV panel can be calculated from the heat balance across the PV cell as follows [25].

$$Q_{in} = mC_{p\_module}\Delta T = mC_{p_{module}}(T_C - T_m) \quad (13)$$

Where is the module back-surface temperature?

It is assumed that the T_m is equal to the surface temperature of the heat exchanger tubes welded to the solar PV cell/panel in close contact with the back surface of each of the PV cells. The heat transferred from the back of the PV cell to the Heat Transfer Fluid HTF flowing in the Heat Exchanger Tubes, as shown in Figure 1, is computed by the following forced heat transfer convection relationship [16,19].

$$Q_{in} = \pi DLh_{water}\Delta T = \pi DLh_{water}(T_m - T_f) \quad (14)$$

Were.
D: Pipe diameter
L: Pipe length
h_{water}: Forced convection heat transfer coefficient
T_f: Fluid temperature

Where the heat transfer coefficient, $h_{water,}$ is approximated as [27].

$$hw = \frac{K_w}{D_H} b_2 Re^n \quad (15)$$

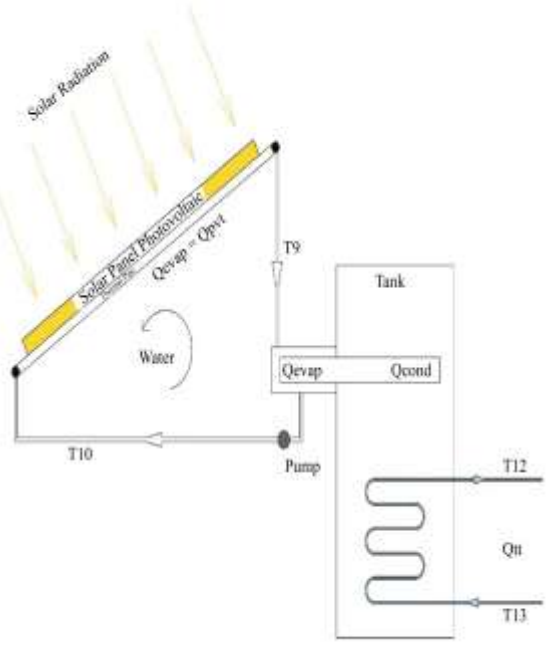

Fig. 1 PV/Thermal-Heat Pipe Hybrid System

Where re is the Reynolds Number, and K_w represents the thermal conductivity of water, b_2 and n are numerical constants

Furthermore, to calculate the heat transfer fluid flow rate, circulating in the heat exchanger tubes, the following equation is used with equations (14) and (15).

$$Q_{in} = \dot{m}_w C_{p\_water}(T_{f+1} - T_f) \quad (16)$$

$\dot{m}_w$: represents the Water flow rate
T_{f+1}: Water temperature at the next element.
C_p: Specific heat of HTF.

The total thermal heat transferred to the HTF is obtained after equations (12) through (16).

$$Q_{th} = (m_{dot} * n_{pipe}) * (T_{sco} - T_{sco}) * Cp_w * \eta \quad (17)$$

Were,

m_{dot}: Mass flow rate per pipe of the heat exchanger tubes welded to the solar PV cell/panel in close contact with the back surface of each of the PV cells.
n_{pipe}: Number of tubes of the heat exchanger welded to the solar PV panel.
T_{sco}, T_{sco}: represent the outlet temperature of the solar collector and the inlet temperature of the solar collector, respectively.
η: Heat exchange efficiency.

This Thermal Heat, calculated by equation (17), is fed to the heat exchanger, where the evaporator section of the heat pipe is placed as shown in Figure 1. This heat is absorbed by the refrigerant in the evaporator section of the heat pipe and transmitted by the natural circulation of the refrigerant to the condenser section of the heat pipe placed in the thermal tank.

1.5. Heat Pipe MODEL

To design a Heat Pipe and attain the required Thermal capacity, the characteristics of the working fluid, the wick, and the container must be determined. For the heat pipe to work correctly, the pressure drop in the fluid flow has to be compensated by the pumping pressure in the wick and the capillarity as prescribed by Tardy and Sami [20], Endale [9], and Reay and Kew [23].

$$\Delta Pp = \Delta Pi + \Delta Pv + \Delta Pg \quad (18)$$

Where ΔPp, ΔPl, ΔPv, and ΔPg are the total pumping pressure, pressure drop for liquid return from the condenser, pressure drop for vapor flow in the evaporator, and gravity head, respectively.

The heat transfer limit for a heat pipe depends on the construction of the heat pipe and the operating environment. The thermophysical properties of the working fluid used and the wick properties determine the design of the heat pipe. The physical phenomena that limit heat pipe heat transfer, such as capillary, sonic, entrainment, boiling, frozen start-up, continuum vapor, vapor pressure, and condenser effects, determine the lowest limit of these phenomena and are considered as a design limit.

The main design limitations were extensively discussed in Tardy and Sami (2009), Fargali et al. (2008), Reay and Kew (2006), and Tardy and Sami (2008). Interested readers in the capillary, sonic, entrainment limit, and boiling limits of the heat pipes are advised to consult the aforementioned references.

The design of a heat pipe depends upon the selection of the working fluid. In selecting the working fluid, several factors are considered. In particular, the working fluid temperature range is an important criterion to be fulfilled. Refrigerants and refrigerant mixtures are widely used as working fluids for low-temperature heat pipe applications because of their lower vapor pressure and boiling points.

In solar applications, the energy conversion and efficiency of heat transfer from the evaporator side of the heat pipe to the condenser side becomes one of the important selection criteria for the working fluid in these particular applications. Hence, the use of a working fluid with higher latent heat is beneficial to the application of the heat pipes. Water and different refrigerants such as R-134a, R-123, R-32, R-125, R-152a, R-1234ze, and R-1234fz are considered in this investigation as working fluids inside the heat pipe to study the impact of working fluids on the behavior of heat pipes, as well as the hybrid system under investigation.

Natural convective heat transfer heat pipes using Two-Phase Thermosyphon principles have been reported in the literature and studied by Endalew [2011] for water-heating applications. On the other hand, Reference [9] also discussed the forced convective condensers under either crossflow or parallel-flow patterns. In the current study, as shown in Figure 1, the Two-Phase Thermosyphon condition in which the condenser section of the heat pipe is directly inserted into the storage thermal tank, where the natural convective heat transfer takes place, and Natural Convection Heat Transfer Mechanisms in the thermal tank are considered in this study. It was assumed that the condensing water flow was stagnant, and there was no temperature gradient along the axis of the heat pipe.

The following gives the energy balance under natural convection heat transfer in the thermal tank for a single control volume of a heat pipe submerged in the thermal tank [9].

$$V_w\, P_w C_w \frac{dTw}{dt} = \pi\, do\, I_{cond} h_{eff}\left(T_{hp} - T_w\right) - U_{tan} A_{tan}\left(T_{hp} - T_a\right) \quad (19)$$

Where V_w represents the water volume in the thermal tank, and $U_{tan}A_{tan}$ is the overall heat transfer coefficient in the thermal tank and the equivalent area in the tank, respectively. In addition, $T_{hp}, T_w\ T_a$ Are the temperatures of the heat pipe, water, and ambient air, respectively?

On the other hand, the effective heat transfer coefficient h_{eff} of the condenser section of the heat pipe can be given by the following,

$$h_{eff} = \frac{1}{h_{cond}} + \frac{1}{h_f} + \frac{\boldsymbol{\delta_{hp}}}{\boldsymbol{\kappa_{hp}}} \quad (20)$$

Where h_f is the natural Heat Transfer Coefficient between the water and the condenser in the thermal tank, δ_{hp} represents the thickness of the heat pipe material, and κ_{hp} Is the thermal conductivity of the working fluid in the heat pipe? In addition, h_{cond} represents the film condensation heat transfer coefficient and can be obtained from the following correlation suggested by references [22] and [9] and using the Nusselt equation.

$$h_{cond} = 0.729\left(\frac{\kappa_l{}^3 \lambda \rho_l(\rho_l - \rho_r) g\, sin\beta}{\mu_l d_i (T_{hp} - T_w)}\right)^{\frac{1}{4}} \quad (21)$$

Where, T_{hp}, T_wRepresent the temperatures of the heat pipe and the water in the tank, respectively, and $\rho_l\ , \rho_r$ Are the liquid and vapor densities of the working fluid inside the heat pipe, respectively? And $\mu_{l,}\ d_i$ Are the viscosity and internal diameter of the heat pipe, respectively?

The following equation gives the Natural Heat Transfer Coefficient h_f between the water in the thermal tank to be heated and the condenser section of the heat pipe, and can also be developed using the Nusselt equation [22, 9].

$$\frac{h_f d_o}{\kappa_l} = 1.09\left(\frac{d_o{}^3 \rho_l{}^2 g\gamma (T_{hp} - T_w) Cp}{\mu_l \kappa_l}\right)^{\frac{1}{5}} \quad (22)$$

Where d_o represents the outside diameter of the condenser section of the heat pipe, and Cp is the specific heat of the working fluid inside the heat pipe? Moreover, γ is the specific heat ratio. μ_l Represents the liquid viscosity of the working fluid.

In the following, the energy and mass balance equations for the condenser section of the heat pipes are considered.

$$Q_{cond\ hp} = h_{eff} * \left(T_{hp} - T_w\right) * d_o * Io * \pi \quad (23)$$

Where Io is the length of the condenser section of the heat pipe?

$$Q_{evap\ hp} = Q_{th} * \eta$$

On the other hand, the thermal energy drawn from the thermal tank and delivered for domestic or industrial use is.

$$Q_{tt} = \eta_{hx} * m_{wQtt} * Cp_w * (T_{12} - T_{13}) \quad (24)$$

Where the m_{wQtt} represents the water Mass Flow Rate circulating between the thermal tank and the user application in question. T_{12} and T_{13} are the supply and return temperatures from the user application, respectively. η_{hx} Is the thermal tank efficiency?

The water mass flow rate for supplying hot water to the user's application is.

$$m_{w_{Qtt}} = \frac{Q_{tt}}{\eta_{hx} * Cp_w * (T_{12} - T_{13})} \quad (23)$$

The efficiency of the solar PV panels can be expressed as follows.

$$\eta_{pv} = \frac{Q_{elec}}{Q_{colector}} \quad (26)$$

Where, Q_{elec} is calculated by equation (4) and, $Q_{colector}$ It is obtained by equation (5).

The Thermal Efficiency of Thermal Energy transferred to the evaporator section of the Heat Pipe is.

$$\eta_{Qth} = \frac{Q_{th}}{Q_{colector}} \quad (27)$$

Where Q_{th}It is calculated by equation (17).

The following equation can be used to obtain the thermal efficiency of the heat pipe.

$$\eta_{hp} = \frac{Q_{cond\ hp}}{Q_{evap\ hp}} \quad (28)$$

Where, $Q_{cond\ hp}$ represents the heat released by the condenser section of the heat pipe and $CapQ_{evap\ hp} = Q_{th} *$ ɳ where Q_{th}calculated by equation (17), and ɳ is the thermal efficiency of the heat exchanger where the evaporator section of the heat pipe is placed.

Finally, the Hybrid System Energy conversion efficiency for harnessing energy from solar energy using thermal panels and heat pipes can be formulated as.

$$\eta_{sh} = \frac{Q_{cond\ hp} + Q_{elec}}{Q_{colector}} \quad (29)$$

Where, Q_{elec} It is calculated by equation (4).

1.6. Numerical Procedure

The energy conversion and heat transfer mechanisms taking place during various processes, solar PV-Thermal and heat pipe, as well as a thermal tank, as shown in Figure 1, are described in Equations (1) through (29). The model presented here is based on mass and energy balances of the individual components of the PV/T hybrid system: PV cell and the heat transfer fluid flowing in thermal tubes welded in the back of the PV panel and driving the heat pipe. This permits to calculation of the Electrical Power output of the Solar Pv Panel, Thermal Energy recovered from the Solar Pv Panel and supplied to the Heat Pipe, Thermal characteristics of the water flow driving the Heat Pipe, and Thermodynamic and Thermophysical properties of the refrigerants in the Heat Pipe and finally, the Hybrid System total characteristics and individual efficiencies in terms of Solar Radiation and other Geometrical Parameters and boundary conditions.

These equations have been solved as per the logical flow diagram presented in Figure 3, where the input parameters of the Solar PV-Thermal conditions, such as Solar Radiation, Ambient Temperature, and Humidity, as well as other independent and geometrical parameters for the solar thermal tube's geometries and heat pipe characteristics, are defined. Dependent parameters were calculated and integrated with finite-difference formulations. Iterations were performed until a converged solution was reached with an acceptable iteration error.

The numerical procedure starts with solar radiation and ambient conditions to calculate the solar PV cell temperature, and PV cell back temperature, as well as heat transfer fluid mass flow characteristics circulating in the thermal closed loop at specified conditions. The Thermodynamic and Thermophysical properties of Heat Transfer Fluid (HTF) were employed to calculate the water flow rate. This is followed by the finite-difference formulations to predict the time variation of the PV cell temperature, the PV back temperature, and thermal heat transferred to the Heat Transfer Fluid, Heat transfer Fluid outlet temperature at the heat exchanger, as well as the water temperature in the thermal tank, and the heat transfer fluid that drives the evaporator section of the heat pipe. This step is followed by the selection of the heat pipe working fluids: refrigerant and refrigerant mixture, operating conditions, and thermodynamic and thermophysical properties of the refrigerant circulating in the heat pipe. Finally, other hybrid system characteristics, such as the thermal and power outputs and individual efficiencies, are calculated, as well as the Hybrid System efficiency at each input condition.

The thermophysical and thermodynamic properties of the refrigerants considered in this study, used in the aforementioned model and needed to close the system of equations, are determined using REFPROP software as per reference [31]. The NIST REFPROP database [31] provides the most accurate thermophysical property models for a variety of industrially important working fluids and fluid mixtures, including those that meet accepted standards. It has proven to be a handy and accurate tool in calculating the thermophysical and thermodynamic properties of the refrigerants, such as pressure, temperature, and enthalpy.

2. Results and Discussion

To solve the aforementioned equations (1) through (29) and taking into account the heat and mass transfer during the solar PV thermal and heat pipe energy conversion processes, the above-mentioned equations were coded, integrated using the finite-difference formulations and solved as per logical flow chart depicted in Figure.2. In addition, for validation, the predicted simulated results for PV solar panel were compared to the data.

In the following sections, we present an analysis and discussion of the predicted numerical results, along with validations of the proposed simulation model. The simulations were performed at fixed temperature differences across the heat exchanger flow pipes bonded to the back of the solar PV panel. However, only results will be presented and analyzed for the temperature difference of 15 °C across the thermal tube. It is worthwhile noting that the numerical simulation presented hereby was conducted under different conditions such as; PV cell temperatures from 10°C through 70°C, ambient temperatures from 10°C through 38°C and solar radiations; 550, 750, 1000 and 1200 w/m^{2}as well as

different refrigerants filled in the heat pipe with lower Global Warming Potential (GWP) such as R134a (HFC 134a), R123 (HCFC 123), R125 (HFC 125), R32 (HFC 32), R152a (HFC 152a), R1234ze (HFO 1234ze), R1234fz((HFO 1234zf). Thermodynamic and Thermophysical properties were obtained using the methodology outlined and presented in reference [31].

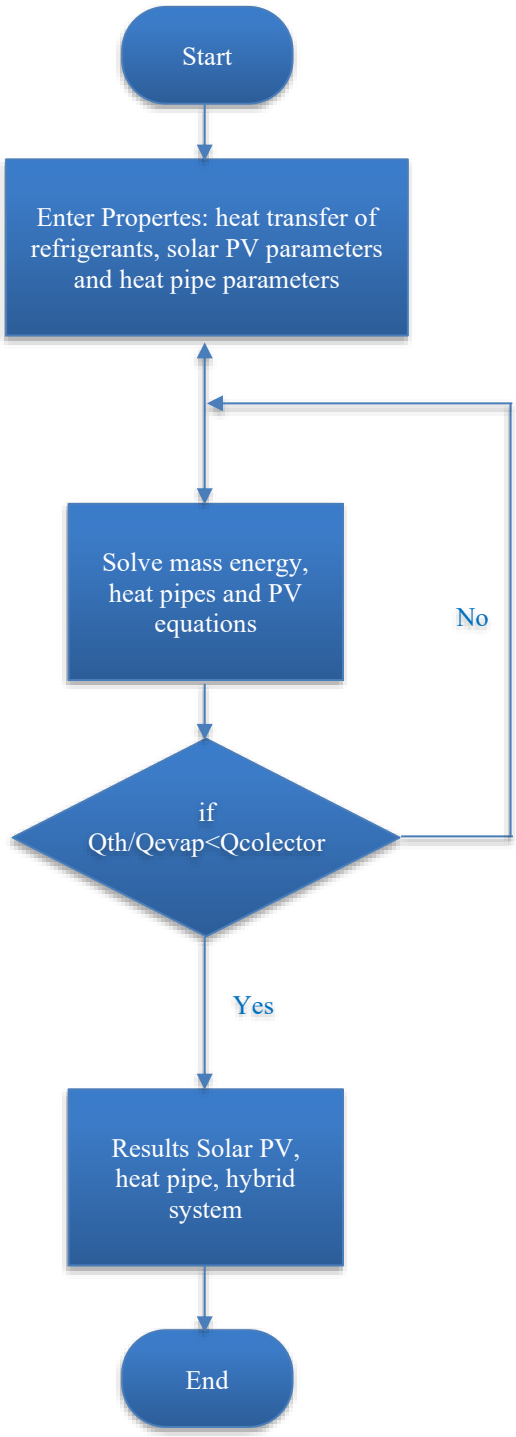

Fig. 3 Logical Flow Diagram

The PV characteristic curves are given in the manufacturer's specification sheet. The PV panel characteristic curves under consideration in this study are obtained from Faragali et al. [17]. Among the parameters used in this study is the total surface area of the PV Module (SP), which is 0.617 m^2, the Total surface area of cells in the Module (Sc) is 0.5625 m2, the Module Efficiency of 12% at reference temperature (298 K), the overall absorption coefficient is 0.73, and the Temperature coefficient is 0.0045 K-1. Interested readers in the full range of values of the other parameters are advised to consult Faragali et al. [17].

It is also assumed in this simulation that the whole panel is covered in PV cells, with no packing material (material used to fill in gaps between the cells on a panel. The PV cells are Commercial-Grade Monocrystalline Silicon Cells with an Electrical Efficiency of 12% and have a Thermal Coefficient of 0.54% [1/K]; however, it depends upon the rated solar radiation [21]. The Thermal Coefficient represents the degradation of PV cell output per degree of temperature increase. The heat exchanger pipes are bonded to the back of the PV solar model without any air gap to ensure complete heat transfer by conduction, Convection, and radiation to the fluid flowing in the thermal pipes. The existing temperatures of heat transfer fluid vary between 25 C° to 75 °C. This Heat Transfer Fluid drives the evaporator section of the Heat Pipe, and the Thermal Heat absorbed from the Heat Transfer fluid evaporates the refrigerant in the evaporator section of the heat pipe. The vapor refrigerant is then circulated by natural Convection and carried to the condenser section of the heat pipe, where it dissipates its Heat Of Condensation to the water in the Thermal Tank.

As per equations (6) through (15), an increase in the PV cell temperature will result in an increase in the back-cell temperature and consequently the fluid temperature due to the heat transfer from solar energy by conduction and Convection as well as radiation, respectively.
Consequently, this increases the thermal heat driving the evaporator section of the heat pipe and increases the thermal energy transferred to the thermal tank.

Furthermore, Figures 4 through 6 show the dynamic behavior of the three critical temperatures in this analysis: PV cell, PV back, and fluid temperatures at different solar radiation levels. These figures support the aforementioned statement that the higher the cell temperature, the higher the back cell and the higher fluid temperatures, as well as the thermal energy delivered to the evaporator section of the heat pipe. It is pretty evident from the results presented in these figures that cell temperatures increase with the increase in solar radiation. This can be interpreted as per equations (1) and (2), where the higher the solar radiation, the higher the energy absorbed by the PV cell and consequently the higher the temperature of the cell until it reaches the design temperature.

Figure 8 presents the thermal heat released from one solar PV panel at different solar radiation and heat pipe temperatures for two heat pipes. The heat pipe temperature is the temperature at which the evaporation and condensation of the working fluid take place. The working fluids filled in the heat pipe were water and the aforementioned refrigerants. The heat balance performed at the Hybrid System presented in Figure 1 suggested that two heat pipes result in an optimized performance of the system in question.

The results presented in this figure for water as a working fluid show that the higher the solar radiation, the higher the thermal energy absorbed by the heat transfer fluid. In addition, at a specific solar radiation, the higher the thermal heat transferred to the transfer fluid and the evaporator section of the heat pipe, the higher the heat pipe temperature.

The Efficiency of thermal Heat released, calculated by equation (27), at different solar radiation and heat transfer fluid temperatures for one solar PV panel with two heat pipes filled with water, is presented in Figure 9.

The thermal heat efficiency is defined as the heat transferred divided by the solar radiation absorbed by the PV panel. It is pretty evident from the results presented in this figure that the higher the solar radiation, the higher the thermal conversion efficiency. It is pretty evident from the results presented in this figure that the higher the solar radiation, the higher the thermal heat released and its efficiency.

Equations (19) through (23) were used to determine the heat released by the condenser section of the heat pipe. In order to analyze the results of this heat release by the condenser section of the heat pipe, Figure 10 has been constructed to show the heat released by the condenser section of the heat pipe filled with water as working fluid and plotted at different solar radiation and heat pipe temperatures. It is pretty clear from the results presented in this figure that the higher the solar radiation, the higher the heat released by the condenser section of the heat pipe. Furthermore, at specific solar radiation, higher heat pipe temperatures result in higher heat released at the condenser section.

The thermal heat transferred to the heat pipe evaporator section, as well as the entering, is plotted and presented in Figure 11 at different solar radiation with the heat pipe using water as refrigerant. This was necessary to examine the impact of the solar radiation on the heat pump's performance. It is pretty clear from the results presented in this figure that the higher the solar radiation, the higher the evaporator entering temperatures, and obviously, the higher the thermal heat transferred to the heat pipe evaporator section. Similar behavior has been observed for the other refrigerants used in the heat pump under investigation. A comparison of the heats released by different refrigerants is discussed elsewhere in the paper.

Figure 11 quantifies the heat released by the evaporator section of the heat pipe using water as the working fluid and at different solar radiation levels. Furthermore, at constant solar radiation, higher heat transfer fluid temperatures result in higher heat absorbed by the evaporator section. Thus, it enhances the heat released by the condenser section of the heat pipe and, consequently, the heat pipe energy conversion efficiency.

The Efficiency of a Heat pipe filled with water as a working fluid can be calculated from equations (27) through (29). Figure 12 has been constructed to demonstrate the Heat Pipe efficiency at different Solar Radiation and Heat Pipe Temperatures. It appears from the results presented in this Figure that the higher the heat pipe temperature, the higher the heat pipe efficiency. However, it was observed that higher solar radiation does not necessarily result in higher heat pipe efficiency. This could be attributed to the fact that higher solar radiation results in higher thermal heat transfer to the heat transfer fluid and consequently to the evaporator section of the heat pipe. However, the thermal capacity, the characteristic of the working fluid, the wick, and the container of the heat pipe determine the condenser section thermal capacity of the heat pipe as per equations (18) through (23) and Tardy and Sami [20], Endale [9], and Reay and Kew [23]. It is believed that the limitations imposed by the aforementioned determine the amount of heat released by the condenser section of the heat pipe. This could result in higher heat losses during the energy transfer process inside the heat pipe at higher solar radiation. Therefore, it is believed that higher solar radiation does not necessarily result in higher heat pipe efficiency. It is important to design the heat pipe based on the site's solar radiation and select the appropriate geometry of the heat pipe to maximize the energy conversion efficiency of the heat pipe at this particular solar radiation.

Further to the aforementioned discussion and the results presented in the Figure.12, Figure 13 has been constructed to present the efficiency of the Hybrid system with a heat pipe filled with water as working fluid at different solar radiations for one solar PV panel and two heat pipes, and discuss the dependency of the hybrid system efficiency on the solar radiation. As previously discussed, and analysis presented on the results of Figure .12, it can be easily pointed out that the higher the heat pipe temperature, the higher the hybrid system efficiency, and also it is believed that the higher solar radiation does not necessarily result in higher hybrid system efficiency.

Figure 14 presents the impact of the different refrigerants under investigation on the thermal heat released by a single heat pipe condenser section of an arrangement of one solar PV panel and two heat pipes core embedded in the thermal tank at 750 w/m2 solar radiation. As previously discussed and stated, the working fluid thermodynamic and

thermophysical properties are very important parameters in determining the amount of thermal heat released from the solar collector, transferred and released by the heat pipe, and used to heat up the thermal tank for further use.

It is pretty clear from the data displayed in this figure that the heat released by the condenser section of the heat pipe is significantly impacted by the characteristics of the heat pipe and the type of working fluid filled in. The data in this illustrative figure shows that the lower the boiling point of the refrigerants, R-32 and R-125, the higher the heat released by the condenser section of the heat pipe. This is attributed to the excellent temperature difference potential between the working fluid inside the heat pipe and the surrounding water in the thermal tank.

In addition, it can also be noticed from this figure that the higher the temperature of the heat pipe, the higher the thermal heat released by the condenser section of the heat pipe. This is one of the most important features of using a heat pipe, where the thermal heat absorbed at the evaporator section of the heat pipe is released in the thermal tank with the help of the natural circulation of the working fluid filled in the heat pipe without any input power and the only source of energy required for this energy conversion process is the solar radiation.

On the other hand, Figure 15 displays the thermal heat released in the thermal tank from the condenser section of the two heat pipes using different refrigerants as working fluids under solar radiation of 750 w/m^2. It can be shown that the lower the boiling point of the refrigerants, such as R-32 and R-125, the higher the heat released by the condenser section of the heat pipe. Other Comments and observations can be made regarding the results presented in this figure, similar to those made about the results displayed in Figure 14.

The dynamic behavior of the fluid flow of the Heat Transfer Fluid (HTF) flowing beneath the PV solar cell is determined by equations (11) and (16) and plotted in Figure 16 under different solar radiations. On the other hand, the results also indicated that the systems stabilized after 1200 seconds, and the desired water flow outlet was reached after this time elapsed, as shown in Figure 7. As expected, the heat transfer fluid mass flow rate increased at higher solar radiation and also stabilized at 1200 seconds. This is because higher solar radiation results in greater thermal energy transferred to the fluid flow at a constant temperature difference across the fluid flow thermal pipe. Consequently, this increases the mass flow rate of fluid. Furthermore, the results presented in this figure also suggest that the fluid flow mass flow rate is quasi-constant during the thermal conversion process.

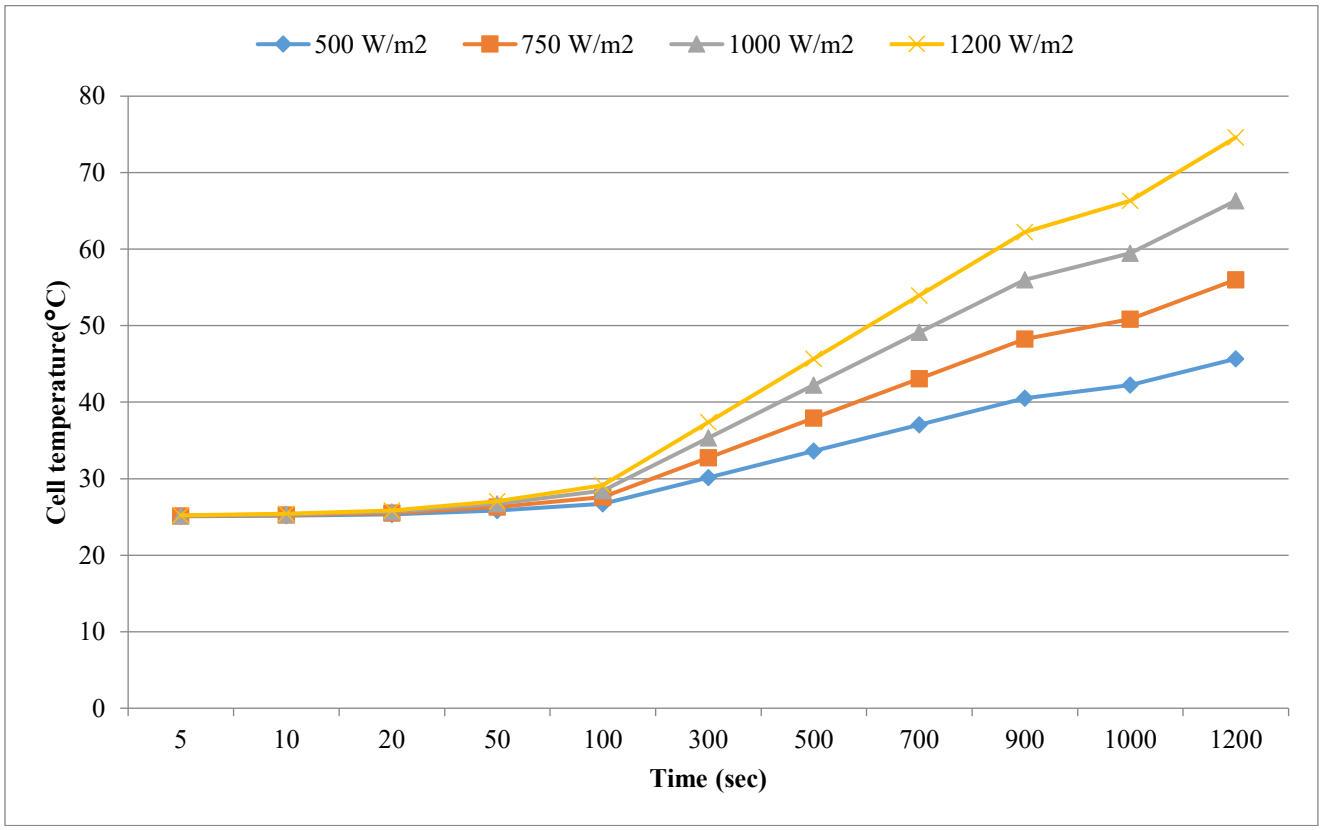

Fig. 4 PV Cell Temperature at different Solar Radiation and a Temperature difference of 15 °C

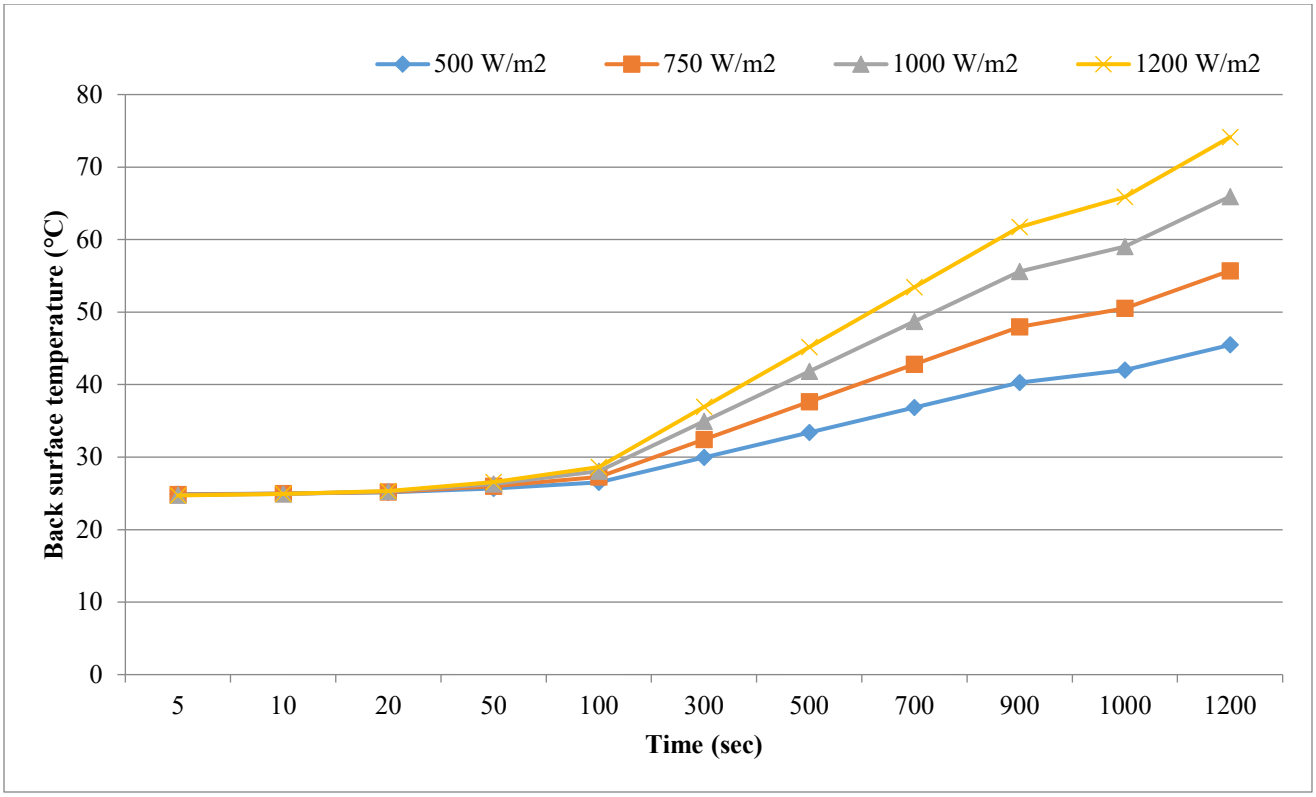

Fig. 5 Back PV Cell Temperature at different Solar Radiation and Heat Exchanger Temperature difference of 15 °C.

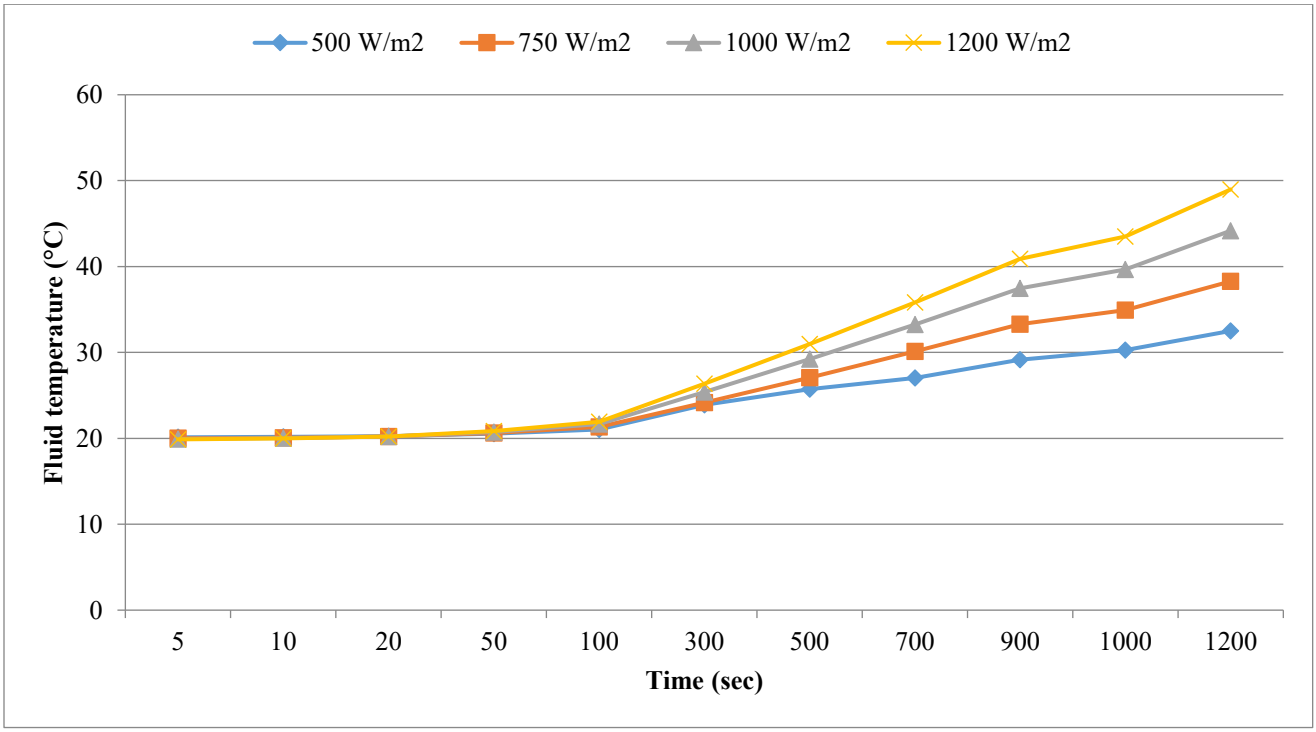

Fig. 6 Fluid Temperature Exiting the Thermal Pipes at a Heat Exchanger Temperature difference of 15 °C

The series of numerical calculations using equations (26) has concluded that the Solar PV efficiency for one solar PV panel at different solar radiation is 22.38% based upon the geometrical configuration of the solar PV panel reported in reference [22].

Furthermore, as shown in Figure 1, this novel concept is intended to enhance the energy conversion efficiency of the PV-Thermal solar hybrid system by utilizing the excess thermal energy dissipated by the conversion process to drive heat pipes to produce domestic hot water, DHW, and obviously enhance the energy conversion efficiency of the Solar Photovoltaic. As PV solar panel efficiency calculations showed, the higher the solar radiation, the higher the solar PV current, and consequently, this increases the solar PV power output; however, the PV solar panel efficiency remains constant at 22.38 % and is independent of the type of working fluid filled in the heat pipes.

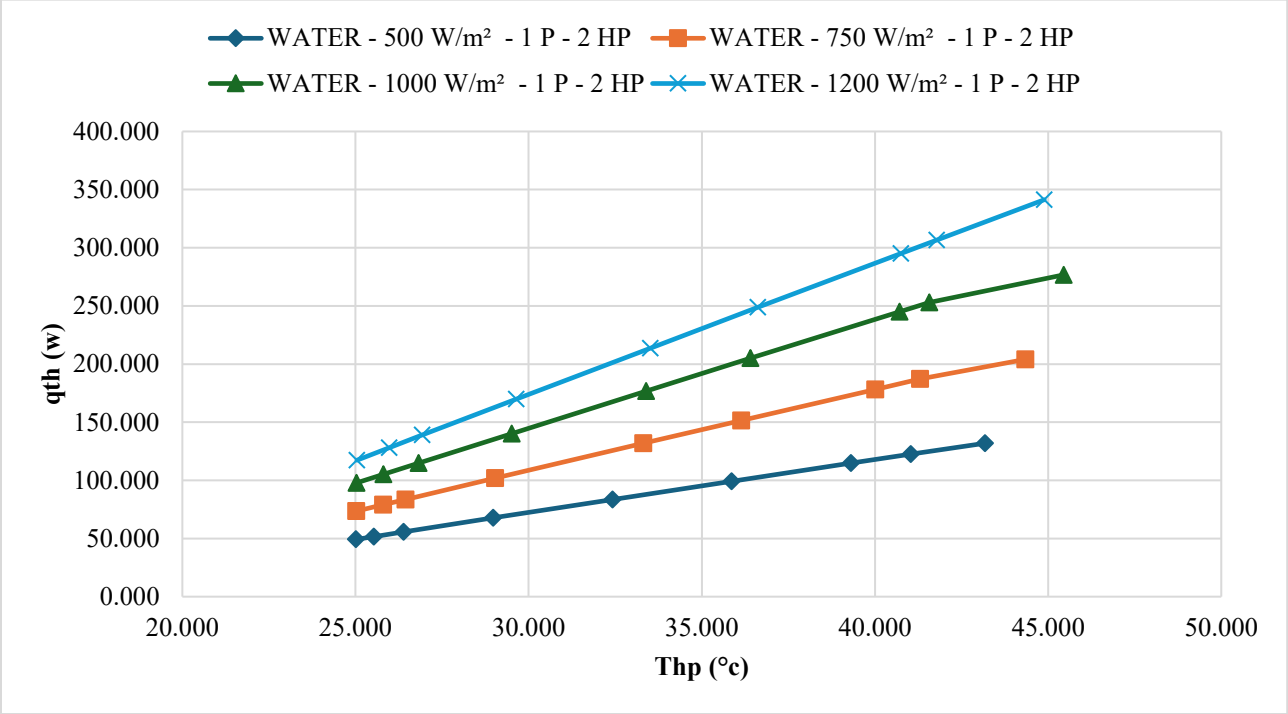

Fig. 8 Heat Released at Different Solar Radiation at One Solar Pv Panel at different Heat Pipe Temperatures and Two Heat Pipes filled with water

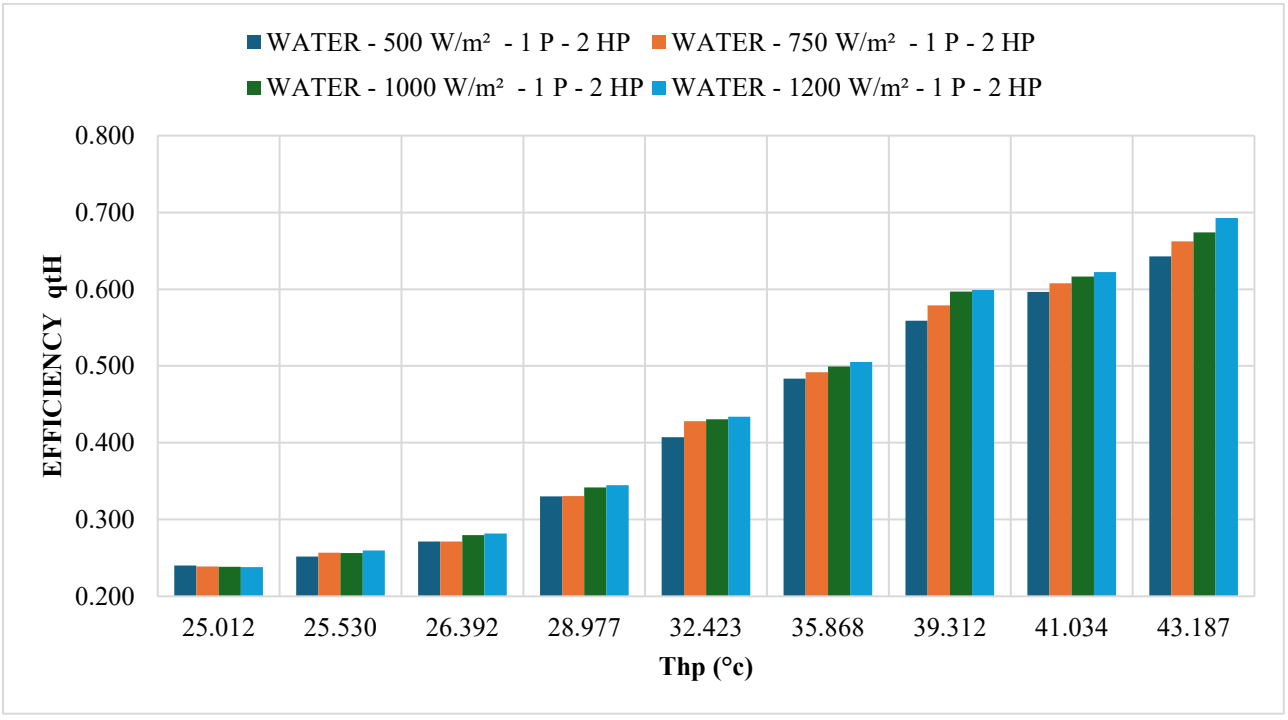

Fig. 9 Efficiency of Heat released at different Solar Radiation and Temperatures at a Solar PV Panel with two Heat Pipes filled with water

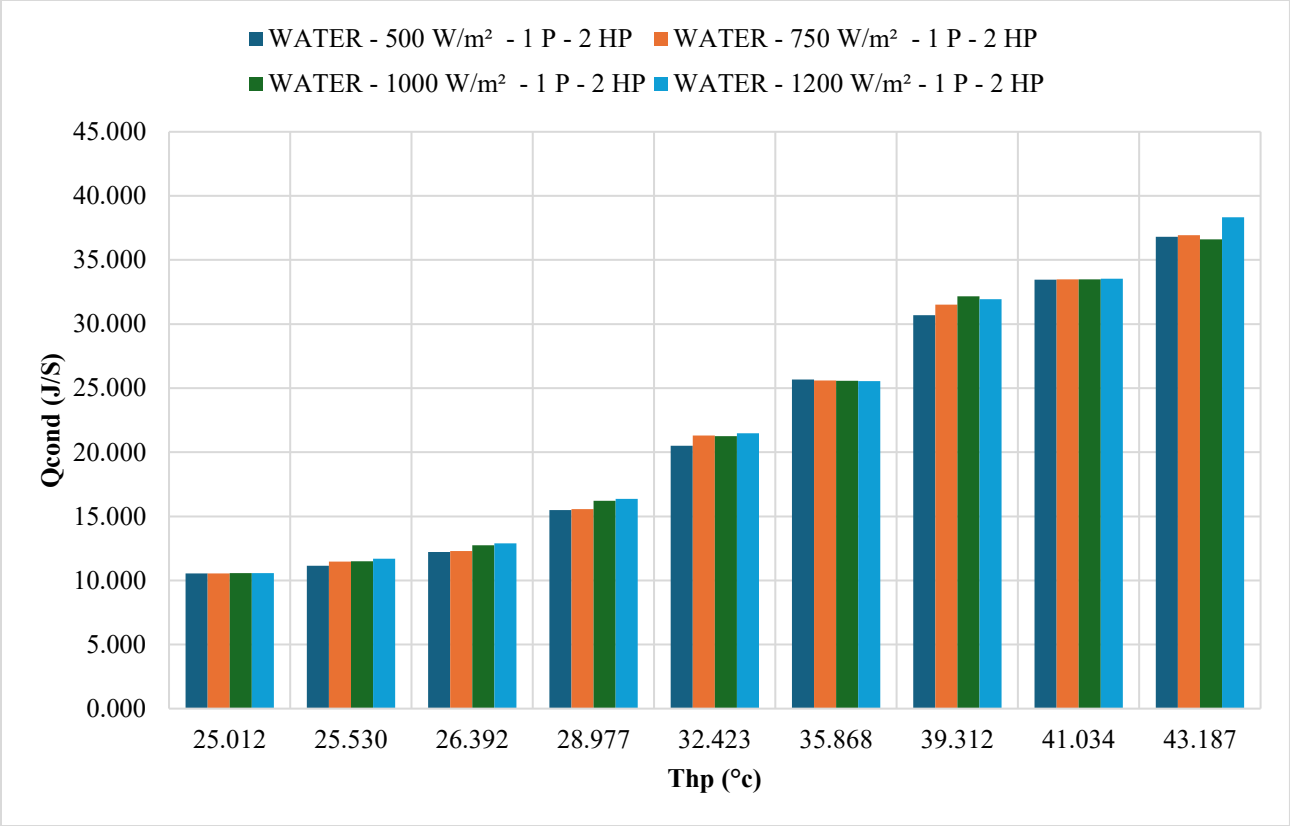

Fig. 10 Heat Released by the Condenser Section of the Heat Pipe Using Water as the Working Fluid and at Different Solar Radiation

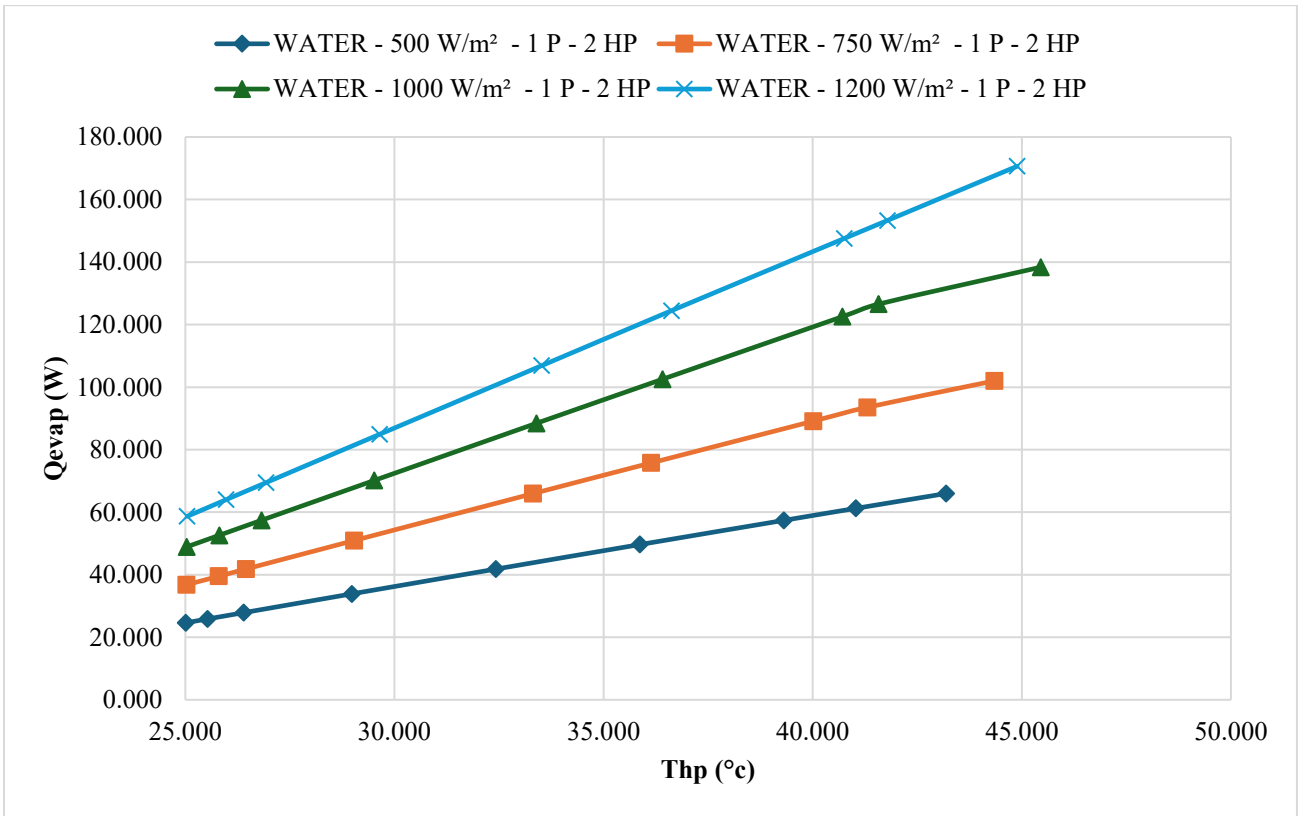

Fig. 11 Heat Released by the Evaporator Section of the Heat Pipe Using Water as the Working Fluid and at Different Solar Radiation

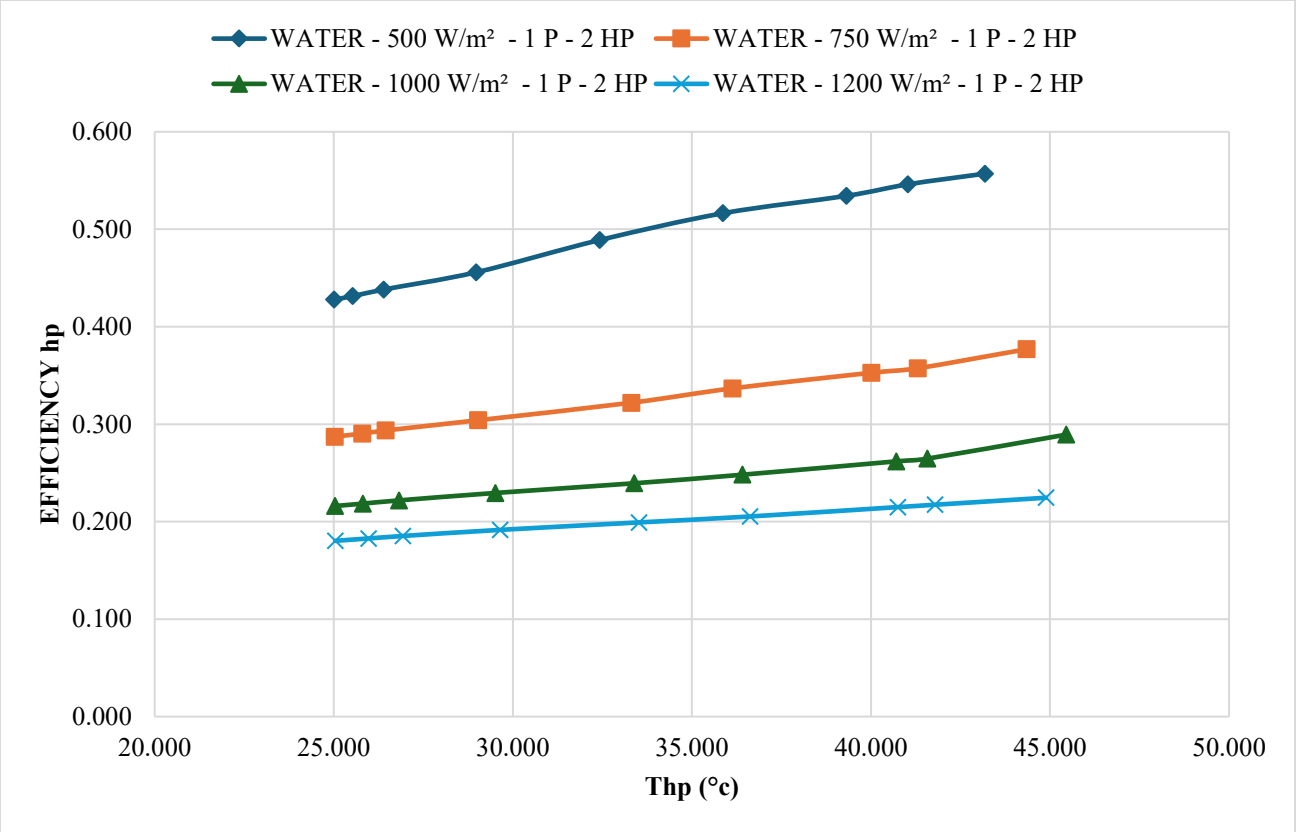

Fig. 12 Efficiency of a Heat Pipe Filled with Water at Different Solar Radiation Levels on One Solar Pv Panel and Two Heat Pipes

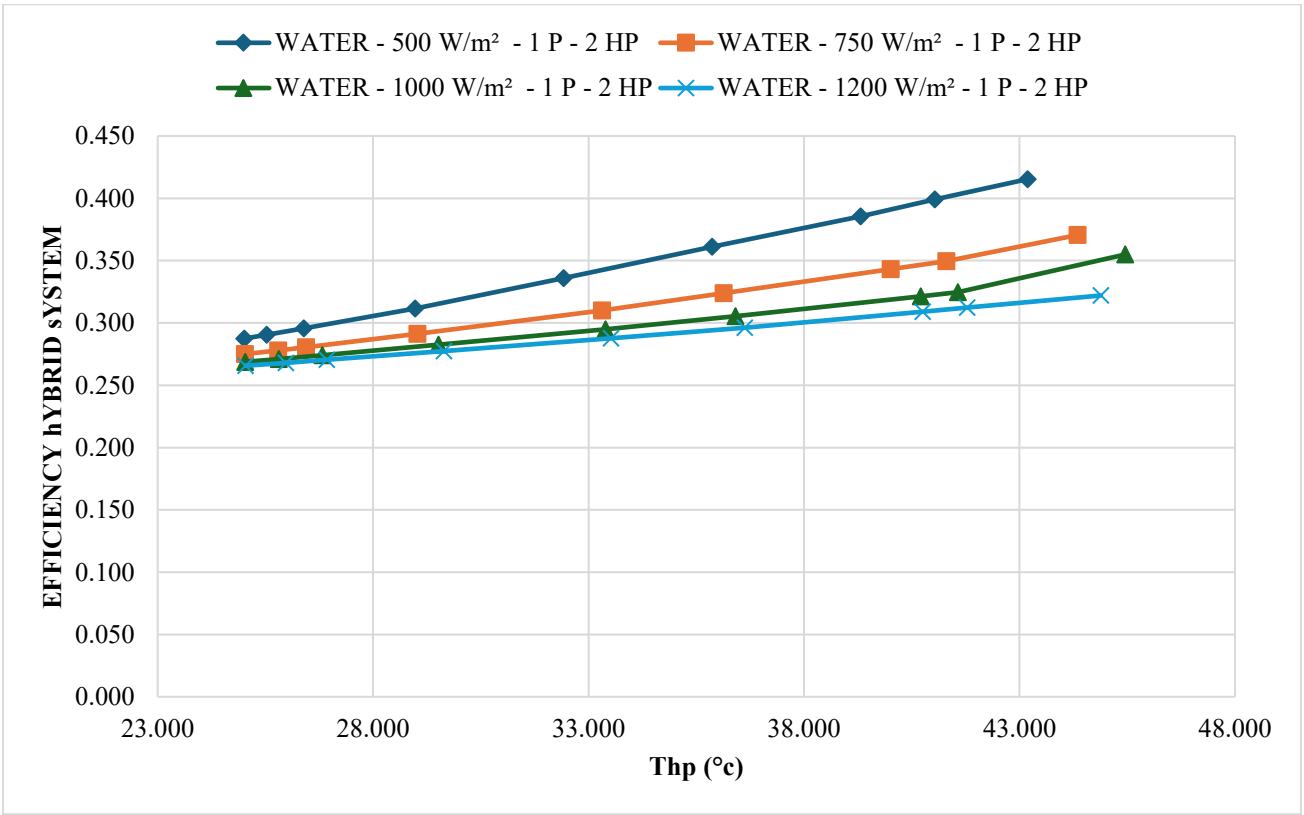

Fig. 13 Efficiency of the Hybrid System with a Heat Pipe Filled with Water at different Solar Radiation at One Solar Pv Panel and Two Heat Pipes.

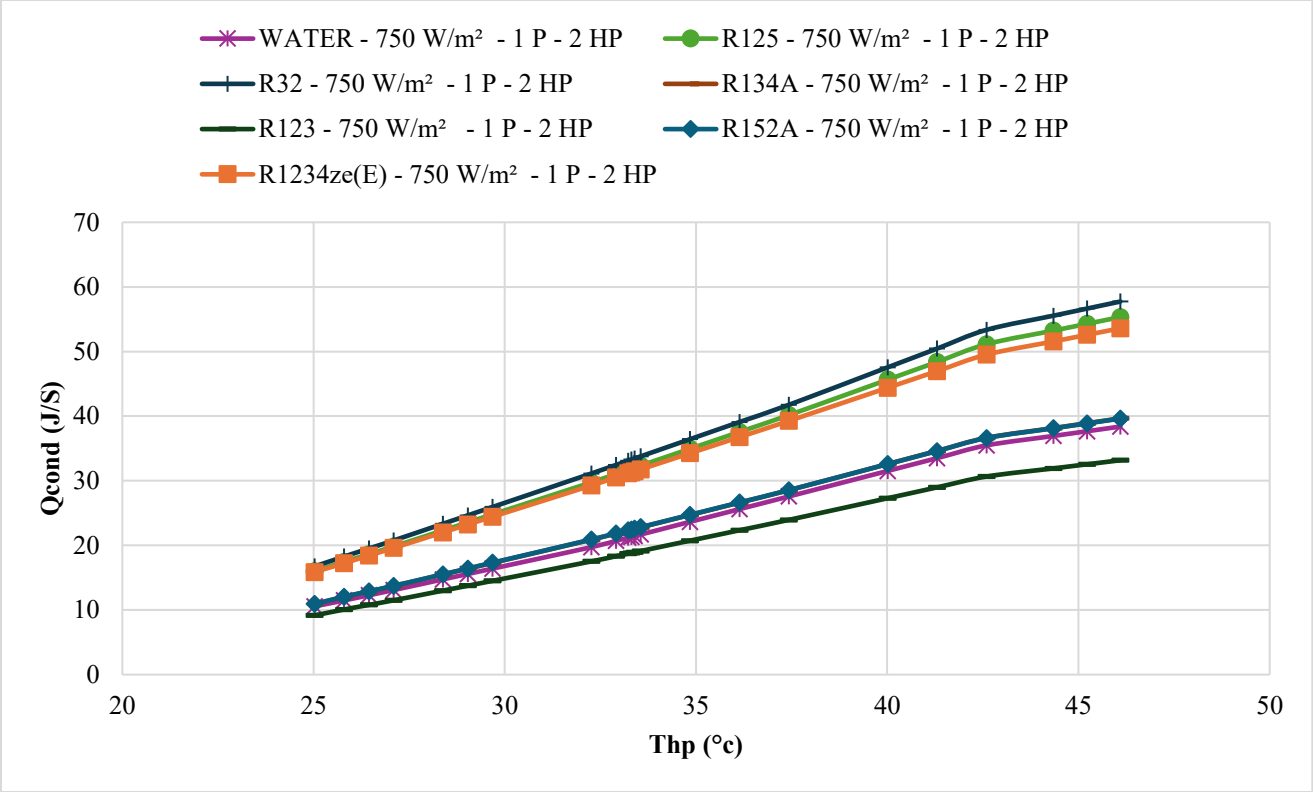

Fig. 14 Heat Released by the Condenser Section of a Single Heat Pipe Using Different Refrigerants as Working Fluid.

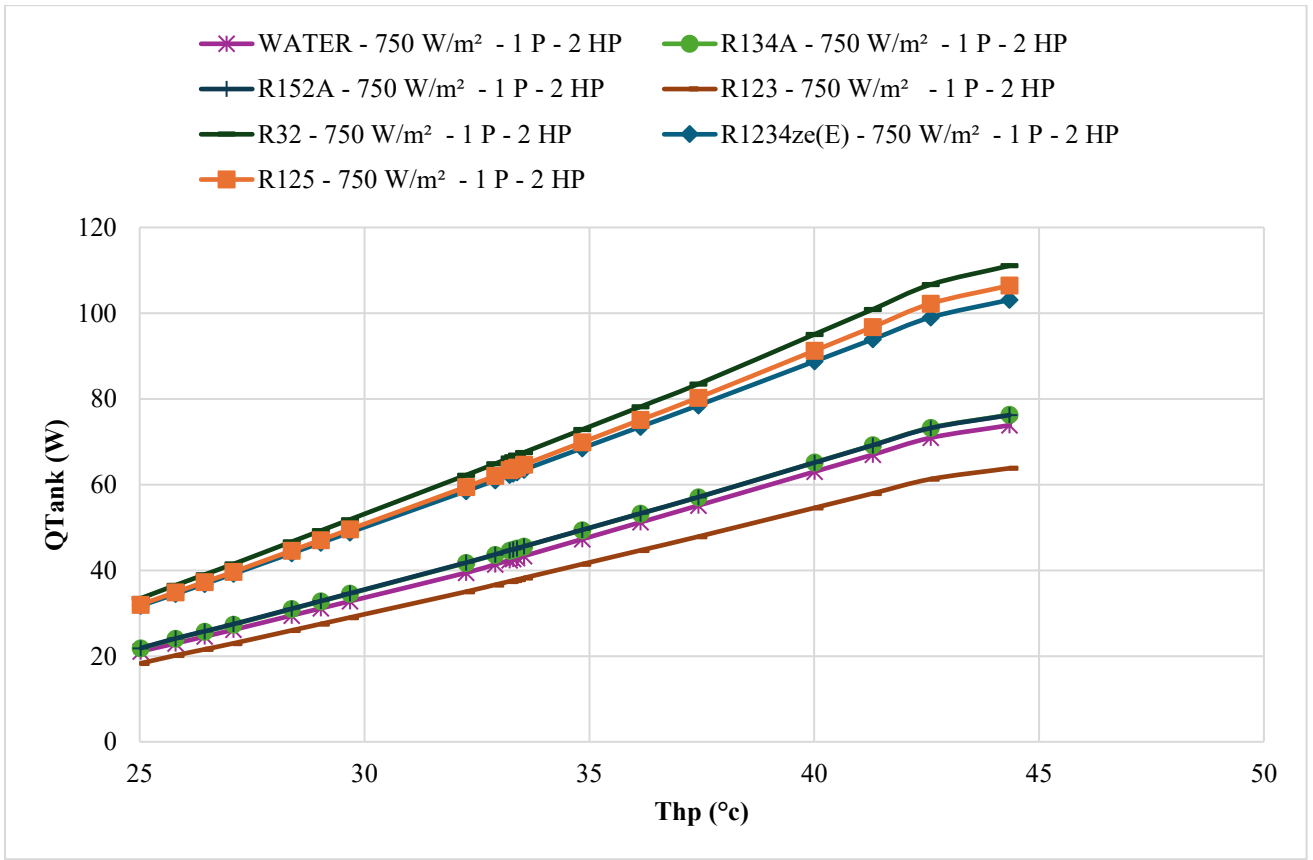

Fig. 15 Heat Released by the Thermal Tank using Different Refrigerants as Working Fluids

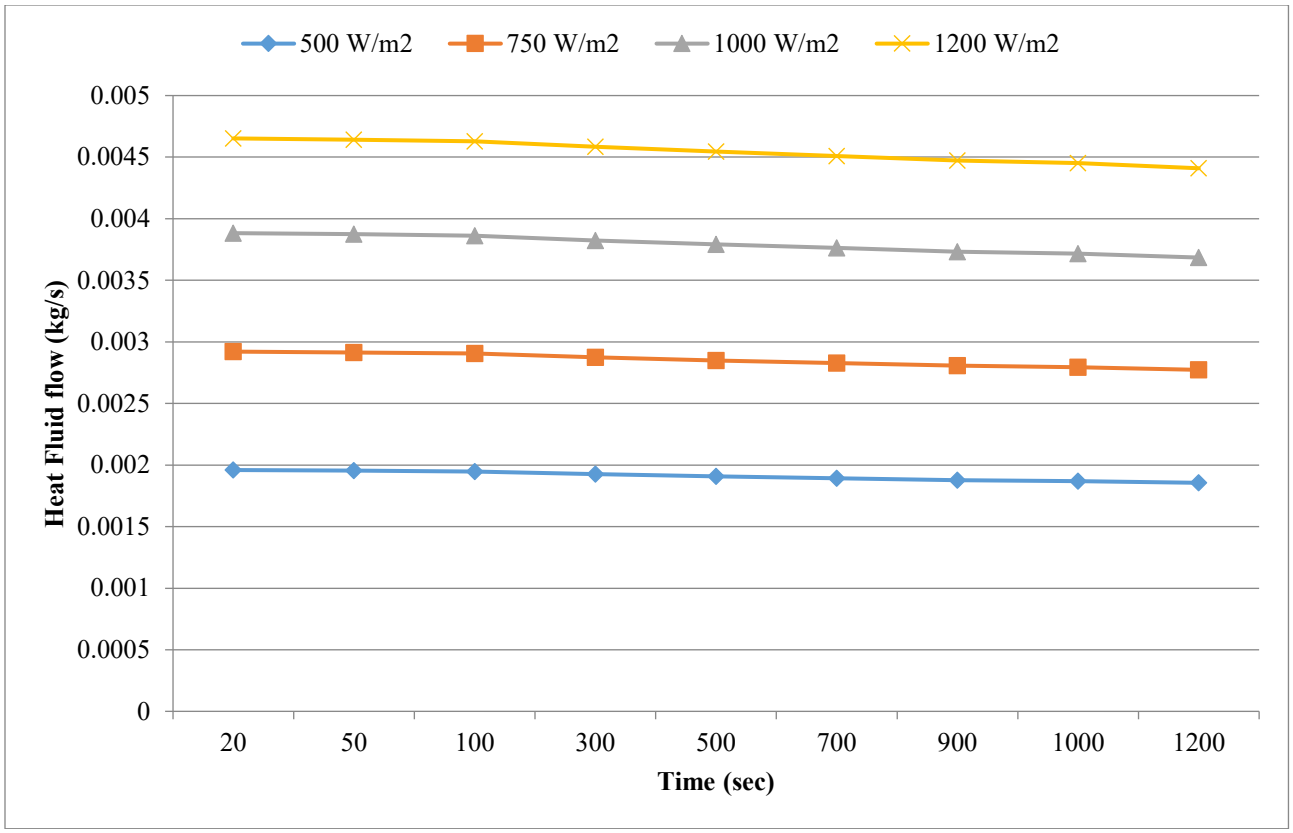

Fig. 16 Heat Transfer Fluid Flow Rate at Different Solar Radiation for One Solar Pv Panel Equipped with Two Heat Pipes

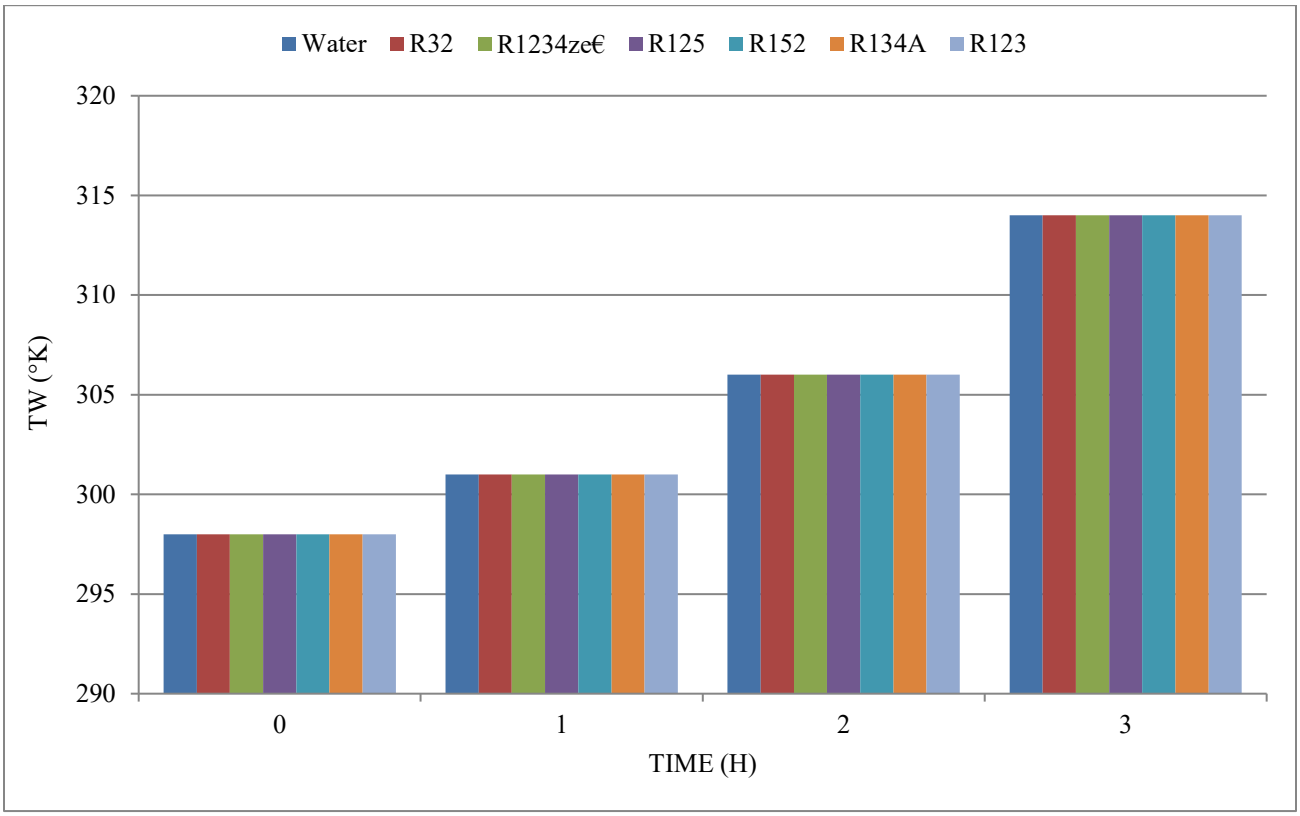

Fig. 17 Water Temperature in the Thermal Tank with the Condenser Section of the Two Heat Pipes Using Different Refrigerants as Working Fluid

© 2026 Seventh Sense Research Group®

Figure 17 presents the water temperature in the thermal tank resulting from the heat released by the condenser section of the two heat pipes using different refrigerants as working fluid. Equation (19) is used to describe the mass and energy balances under natural convection heat transfer in the thermal tank for a single-control volume of heat pipe submerged in the thermal tank [9] and is used to calculate the water temperature plotted in this figure. The results presented in this figure clearly demonstrate that there is no significant impact of the working fluid type filled in the heat pipe on the water temperature. This can be attributed to the fact that the difference between the second and third terms of equation (19) is quasi-independent of the type of refrigerant filled in the heat pipe. However, as shown in Figure 16, the amount of thermal heat transferred into the thermal tank depends upon the type of refrigerant filled in the heat pipe.

Furthermore, examining the results presented in Figures 11 through 17 clearly indicates that the higher the solar radiation, the higher the evaporator temperatures and obviously the higher the heat release from the heat pipe condenser.

Figure 18 has been constructed to show the profile of water temperature in the thermal tank under different solar radiations, 500 through 1200 w/m^{2,} with water as a working fluid filled in the heat pipe. It is evident from the results displayed in this figure that the higher the solar radiation, the higher the water temperature in the thermal tank. This is attributed to the fact that the higher the solar radiation, the higher the thermal energy transferred to the evaporator section of the heat pipe, and consequently to the condenser section of the heat pipe and the thermal tank. It is pretty important to the designer of this system to properly select the site where the solar radiation is the highest to benefit from the higher thermal energy transfer to the water in the thermal tank, and obviously, the higher thermal efficiency of the system in question.

Also, the data shows that for water filled in the heat pipe, the higher the solar radiation, the higher the water temperature in the thermal tank, which is supplied to domestic or industrial demand. Similar behavior has been observed for the other refrigerants used in the heat pump under investigation. A comparison of the heats released by different refrigerants is discussed elsewhere in the paper.

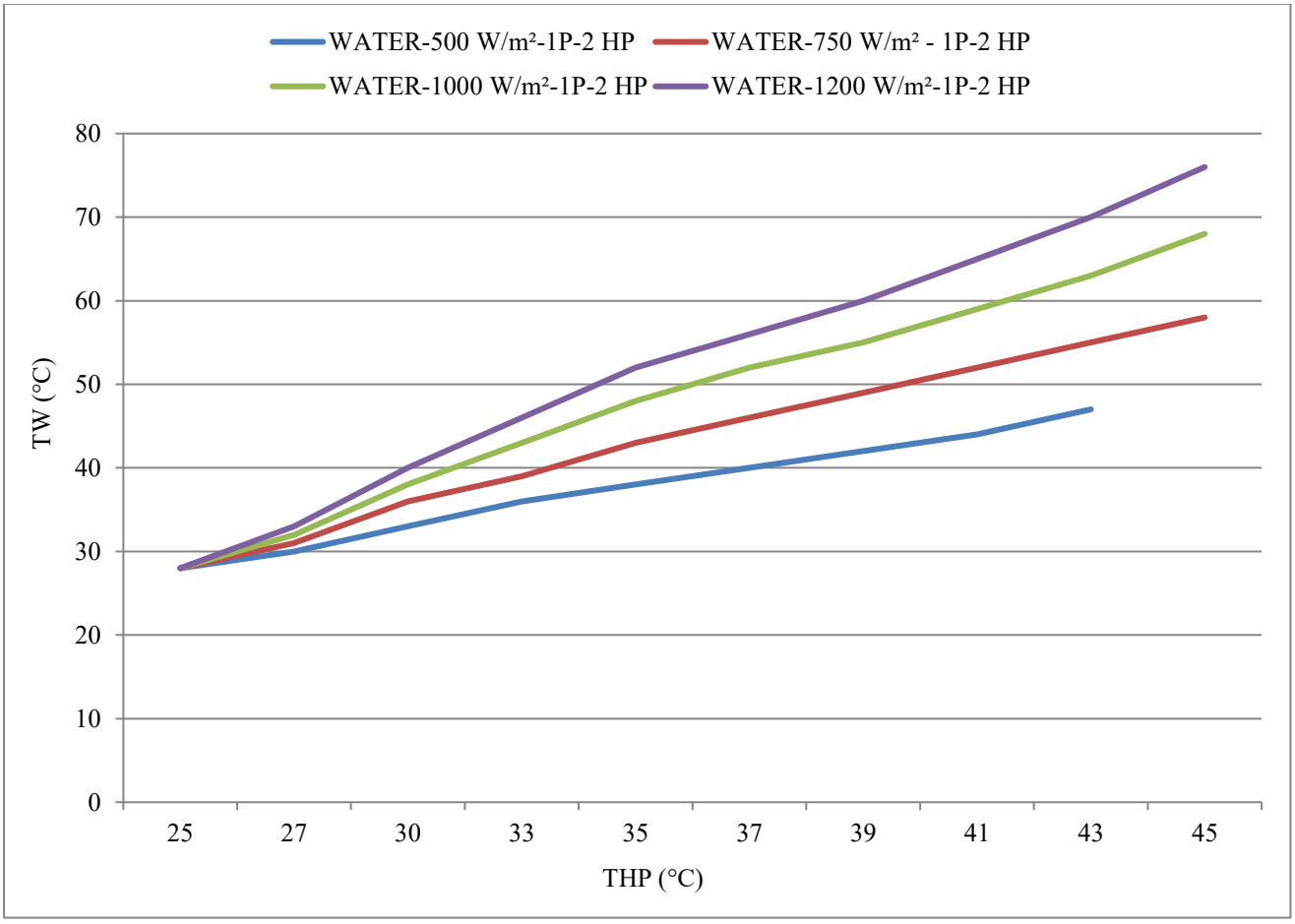

Fig. 18 Water Temperature in the Thermal Tank as a Function of the Heat Pipe Temperature

This is an open access article under the CC BY-NC-ND license (http://creativecommons.org/licenses/by-nc-nd/4.0/)

© 2026 Seventh Sense Research Group®

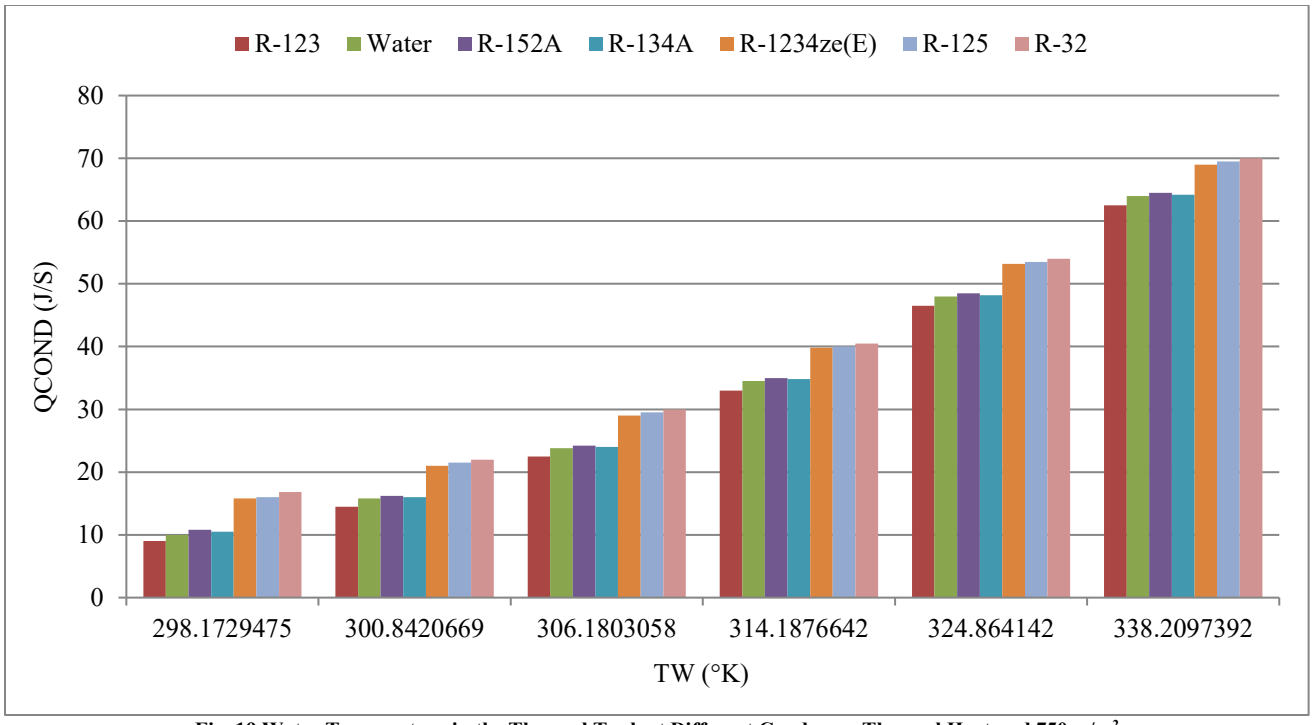

Fig. 19 Water Temperature in the Thermal Tank at Different Condenser Thermal Heat and 750 w/m^2

On the other hand, Figure 19 displays the water temperature in the thermal tank at different heat releases by the condenser section with two heat pipes using different refrigerants as working fluid at solar radiation of 750 w/m^2. It is evident from this figure that the higher the thermal heat released by the condenser section of the heat pipe, the higher the water temperature in the thermal tank. In addition, the data displayed in this figure also demonstrates that refrigerants R-32 and R-125 used as working fluids in the heat pipe have the highest thermal energy released by the condenser and also the highest water temperature in the thermal tank. This is attributed to the significant difference between the boiling point of those refrigerants and the heat pipe temperature. It was also observed that R-1234zef induces higher water temperatures. It is also worthwhile noting that similar behavior has been observed with other solar radiation, namely, 500, 1000, and 1200 W/m^2.

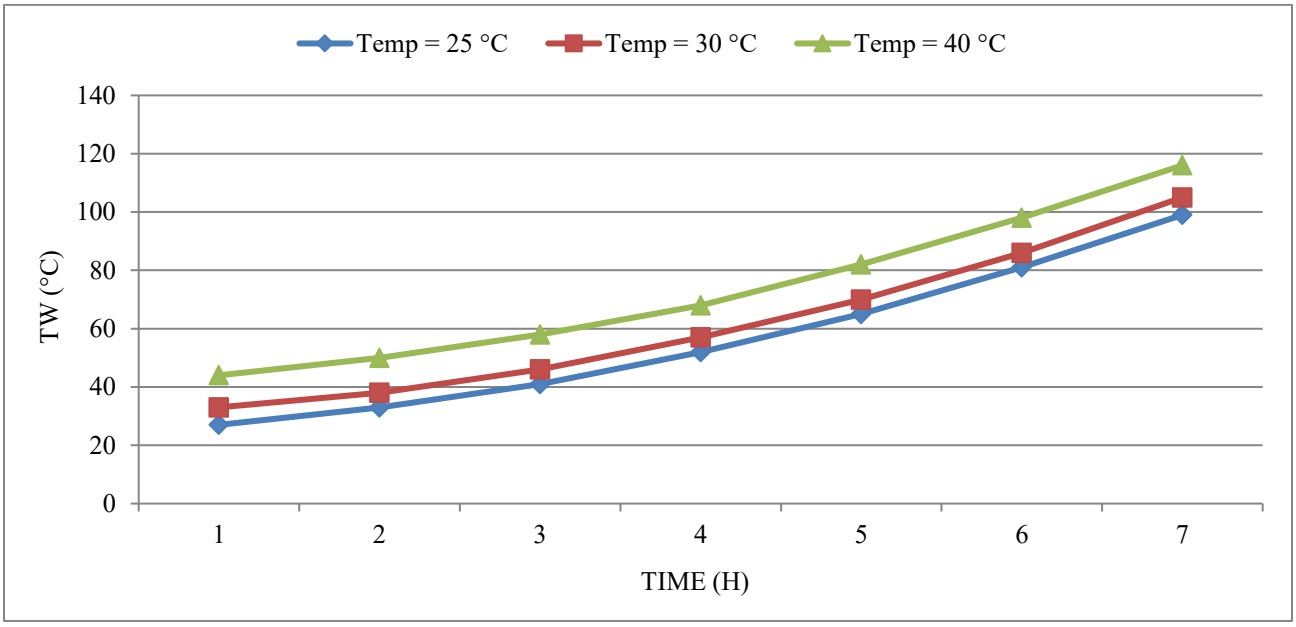

Fig. 20 Water Temperature Dynamic Profile in the Thermal Tank

This is an open access article under the CC BY-NC-ND license (http://creativecommons.org/licenses/by-nc-nd/4.0/)

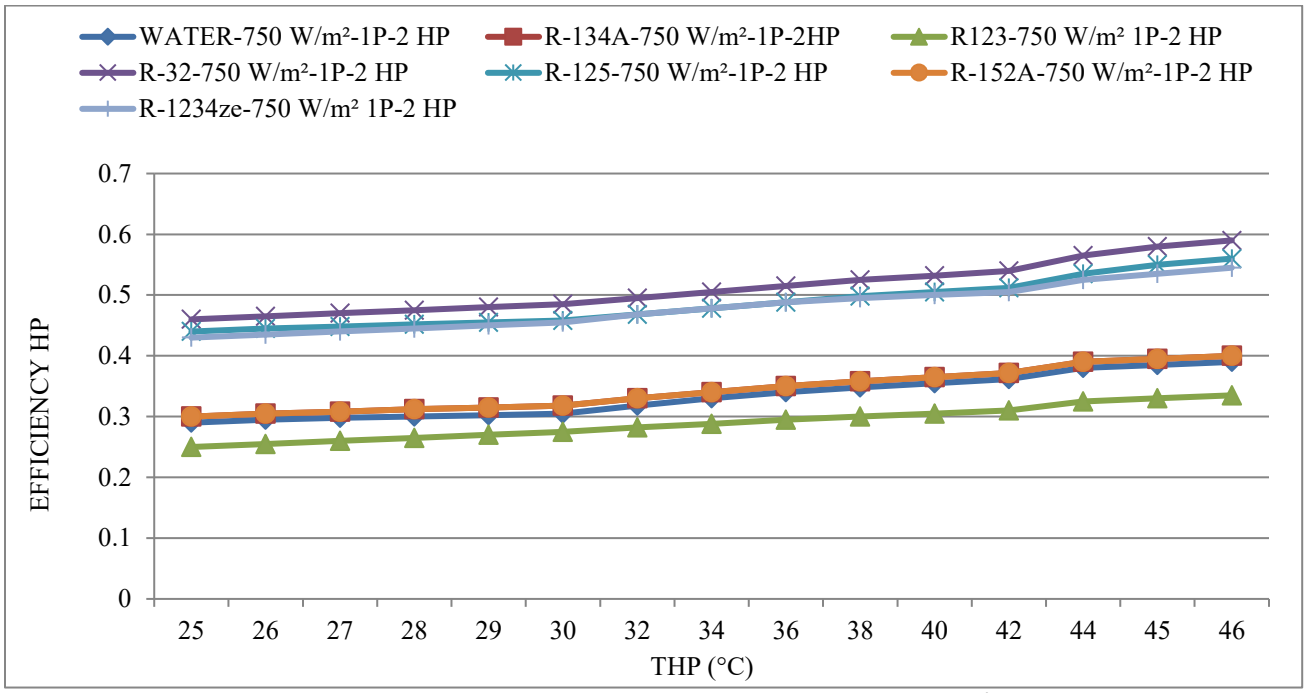

Fig. 21 Heat Pipe Efficiency at Different Working Fluids and at 750 w/m²

The dynamic behavior of the water temperature in the thermal tank is plotted in Figure 20 minutes against time for different supply water temperatures from the solar collector. It is pretty clear from the data presented in this figure that the higher the supply temperature from the solar collector, the higher the water temperature in the thermal tank. In addition, it can be pointed out that the water temperature in the thermal tank for domestic or industrial use can be reached after 5 hours, depending on the solar collector's supply temperature. AS previously discussed, the higher the solar radiation, the higher the water temperature of the solar collector; therefore, the higher the solar radiation, the higher the water temperature in the thermal tank.

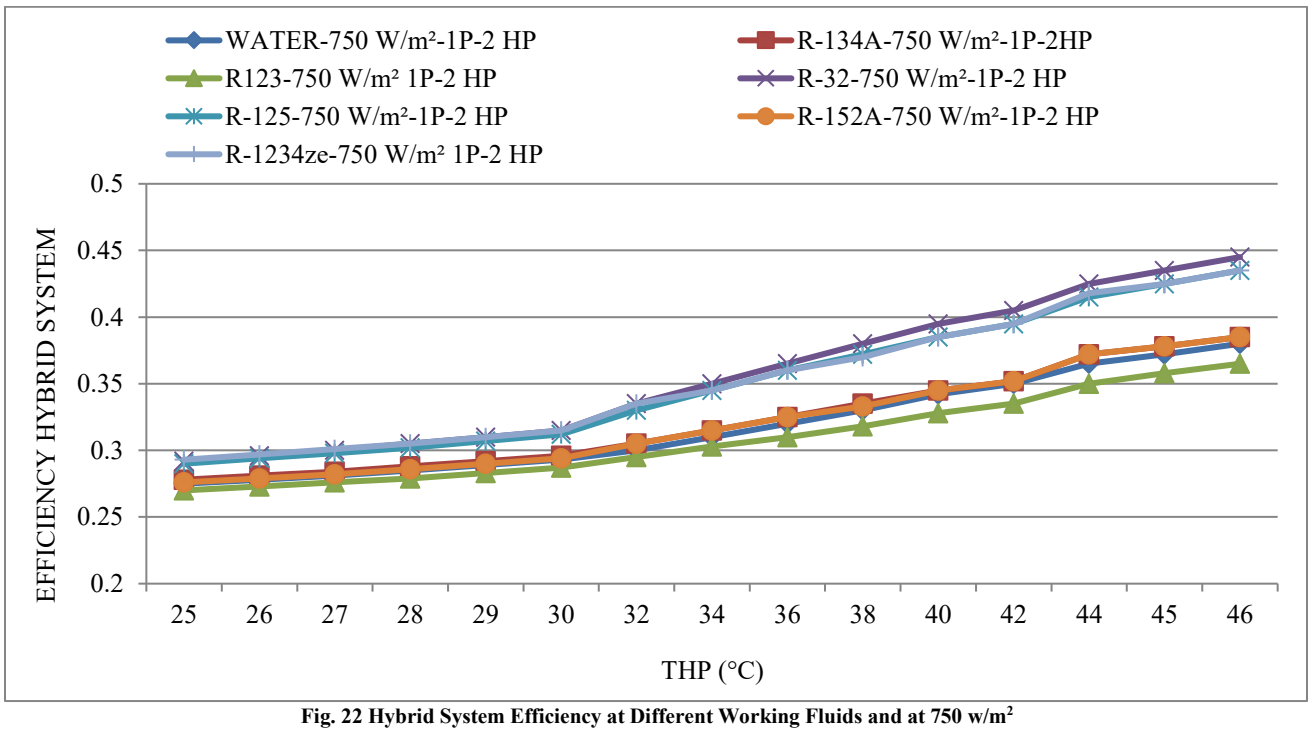

Fig. 22 Hybrid System Efficiency at Different Working Fluids and at 750 w/m²

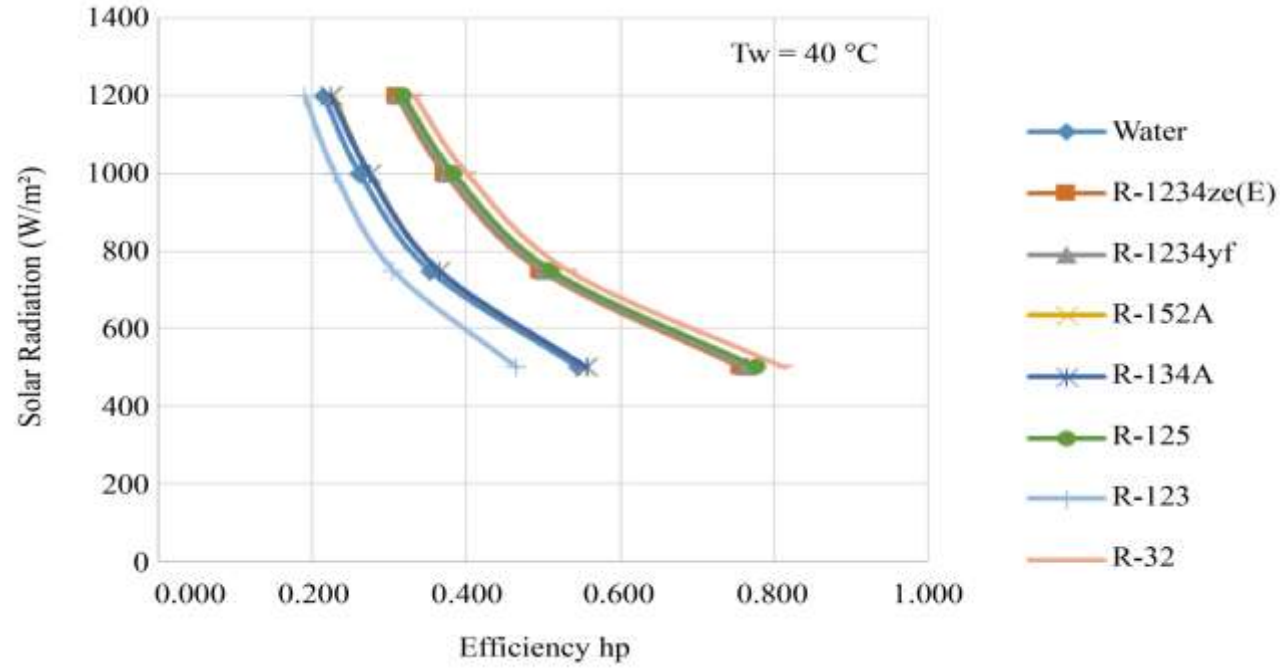

Fig. 23 Heat Pipe Efficiency at Different Working Fluids.

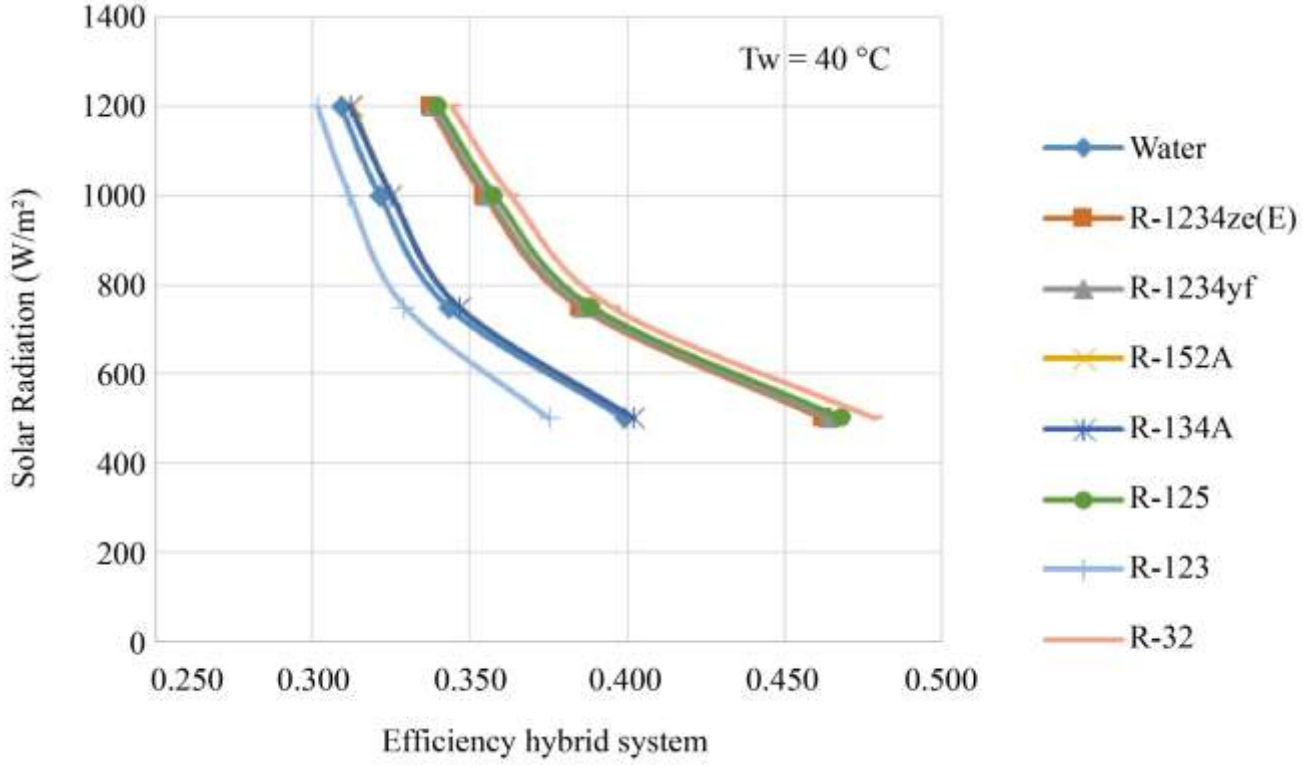

Fig. 24 Hybrid System Efficiency at Different Working Fluids

Another two important characteristics of the Solar PV-Thermal System integrated Heat Pipe are presented in Figures 23 and 24, where the heat pipe and hybrid system efficiencies are shown at different solar radiation levels. It should be noted that the hybrid efficiency of the hybrid is defined by the amount of electrical power and thermal energy released at the thermal tank side for further use, divided by solar radiation. The data presented in these figures show that the higher the solar radiation, the higher the efficiency of the heat pipe and hybrid system.

However, the results displayed in these figures also show that the higher efficiencies of the heat pipe and hybrid system were observed with R-32 and R-125 used as working fluids in the heat pipe. The data displayed in this figure clearly shows that among the refrigerators under investigation, R-125 and R-32 have the highest thermal energy delivered to the thermal tank. This is significant, and therefore it is recommended that R-125 and R-32 be used as working fluids in the heat pipe for this application.

As previously discussed, this is because higher solar radiation levels lead to greater heat losses. Because those refrigerants have a low boiling point of those refrigerants, heat transfer is faster and consequently impacts system efficiency. It is worthwhile mentioning that similar behavior has been observed for the other refrigerants used in this investigation. However, the observed behavior in the aforementioned figures is attributed to the heat losses in the heat transfer process and the thermal tank as reported by reference [32].

Furthermore, in order study the impact of the Number of Solar Pv Panels, Figure 25 has been constructed where the thermal heat released in the thermal tank generated by 5 and 10 solar PV panels was displayed at 750 solar radiation W/m^{2}and at the most promising refrigerants R-125 and R-32 filled in the heat pipe that yield the maximum efficiency of the hybrid system among the other refrigerants under investigation.

This is attributed to the fact that the characteristics and thermodynamic properties of R-125, R-32, and R-407C are the main drivers of the hybrid system's high efficiency. It is evident from the data presented in this figure that the greater the number of solar PV panels, the greater the heat transferred to the water in the thermal tank from the condenser section of the heat pipe. Also, the data presented in this figure showed similar trends to those displayed previously of the thermal heat released by the condenser section of the heat pipe.

The designer of the PV-Thermal integrated heat pipe should consider PV panel features, cell temperatures, local solar radiation, ambient conditions, and refrigerant properties when making decisions.

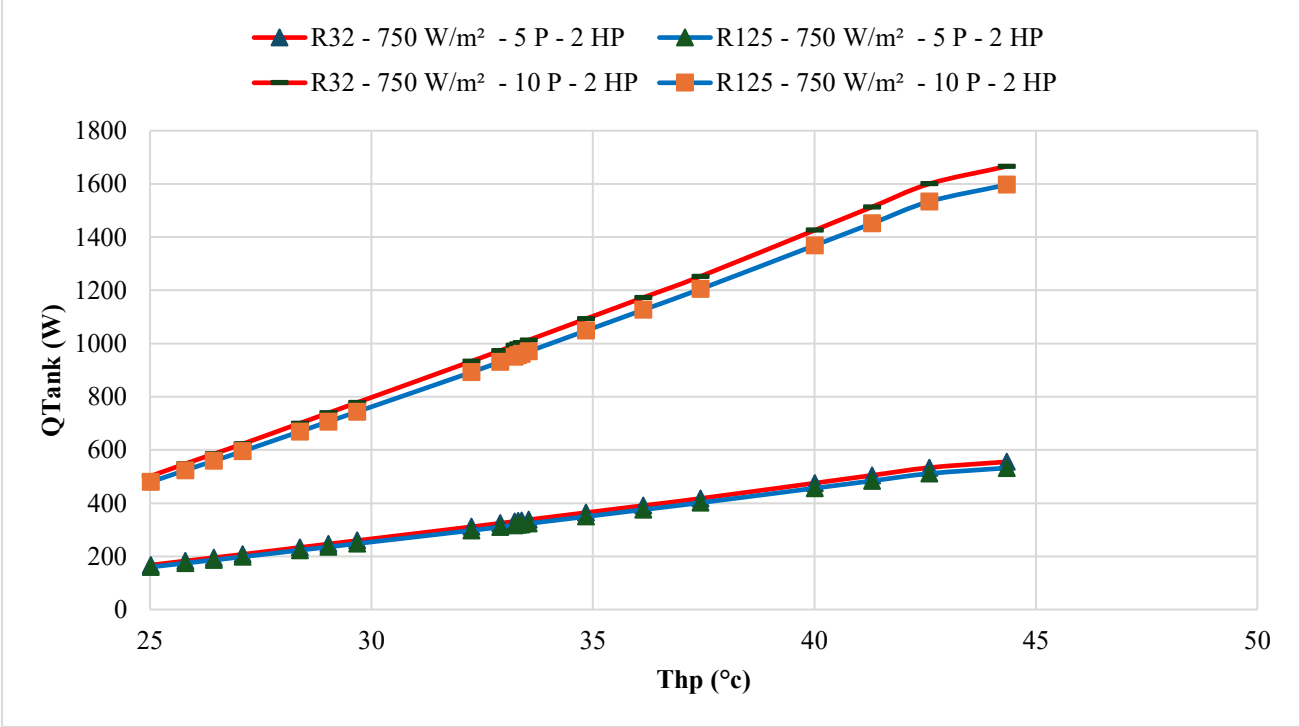

Fig. 25 Thermal Energy Released in the Thermal Tank at Different Numbers of Solar Panels

2.1. Model Validation

To validate the numerical model prediction describing the novel hybrid system under investigation in Equations (1) through (29), only data available in the literature for the solar PV panel and related systems were used for comparison. In the following sections, we discuss the model validation and present the different comparisons. Furthermore, as has been presented in the aforementioned discussion, the basic prediction of the model performance is based upon the determination of the PV Solar Panel characteristics, Cell Temperatures, and Heat dissipated from the PV Solar Panel. Therefore, it was felt that the PV solar model validation

should show strong confidence in the results predicted by the model. Therefore, we have constructed Figures 25 and 28 to compare the proposed model prediction of the PV solar panel and the PV Thermal parameters with the data presented in the literature on the solar PV, namely references [17, 22, and 30]. In particular, as shown in Figure 26, it is pretty apparent from the comparison presented in the figure that the model prediction fairly compares with the data of the dynamic PV cell temperature presented by Faragali et al. [17]. The comparison presented in this figure also showed that the model and data have the same trend as the data; however, some discrepancies exist. It is believed that the discrepancies are because Faragali et al. [17] did not provide full disclosure of the various parameters used in equations (6) through (9), and Reference Rajapakse et al. [30] had to be consulted on the various missing parameters in Faragali et al. [17]. However, as pointed out in references [8, 12, and 17], taking into account the complexity of the PV cell temperature phenomena and its thermal behavior, we feel that our model fairly predicted the PV cell dynamic profile.

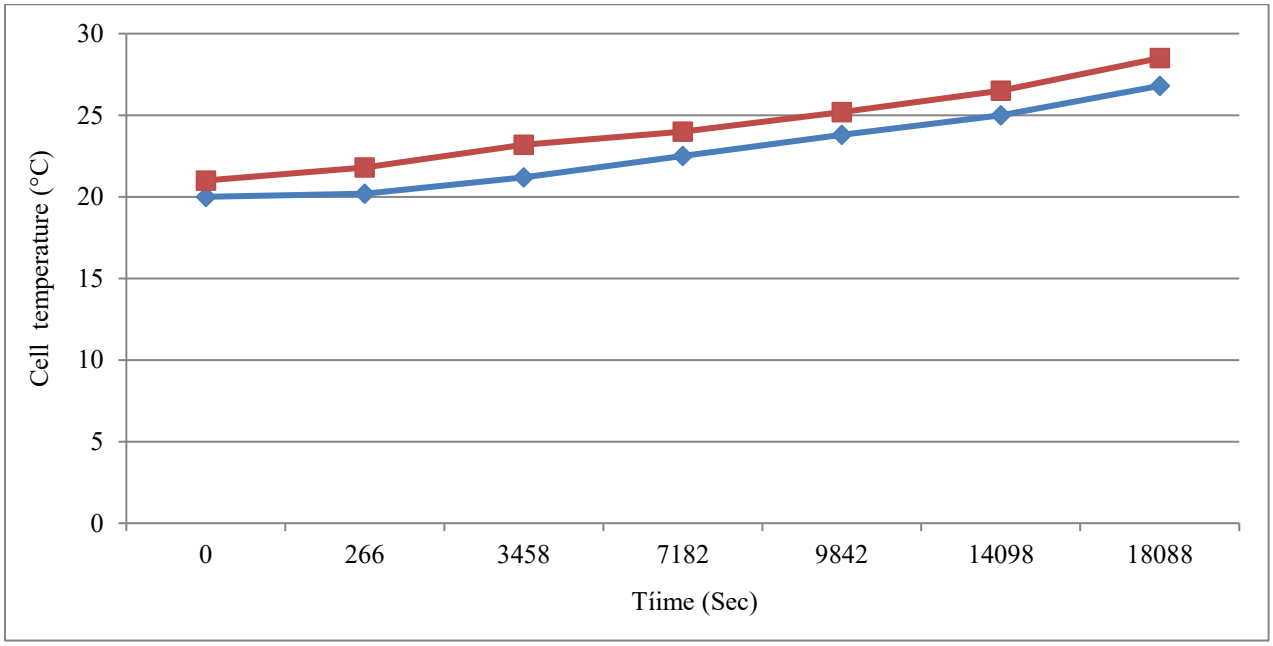

Fig. 26 Model's Validations for Cell Temperature [17]

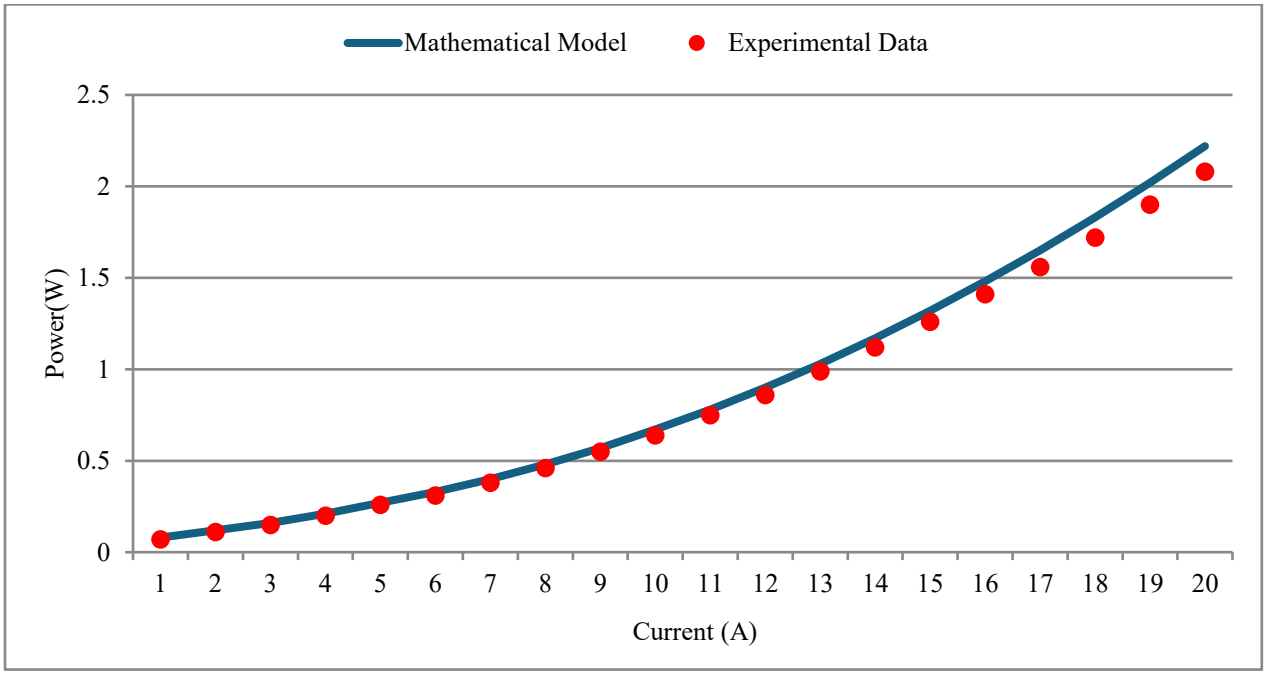

Fig. 27 Comparison Between Model and Experimental Data [17, 30]

© 2026 Seventh Sense Research Group®

Furthermore, Figure 27 shows a comparison between the model's prediction and experimental data presented in [17, 30], where the numerical prediction of the aforementioned Solar Pv Model of the characteristics of the Solar Pv Panel, power at different amperages that vary with solar radiation, is displayed. This figure shows that the present model accurately predicts Solar PV characteristics. Since the present model prediction is an extension of the Solar Pv Model and the work of Sami and Campoverde [27], we strongly feel that the current model is reliable.

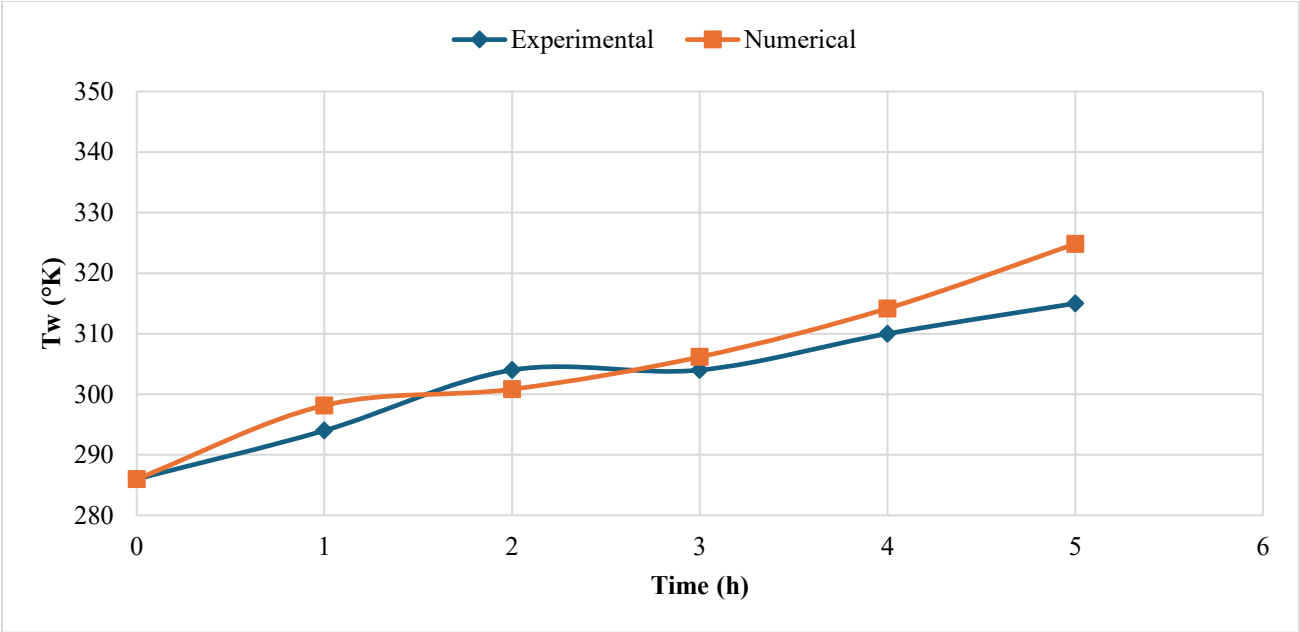

Fig. 28 Comparison Between Model and Experimental Data [9]

Finally, the comparison displayed in Figure 28 between the model's prediction of the water temperature in the thermal tank and the experimental data reported in reference [9] demonstrated clearly that our model predicted the dynamic data of the water temperature in the tank where the condenser section of the Heat Pipes was placed. It can also be noticed that some discrepancies exist between the model's prediction and the data, which are attributed to the heat losses and the calculation of the Heat Transfer coefficient in the thermal tank.

3. Conclusion

The energy conversion equations describing the mass and energy balances have been developed, integrated, and solved to predict the dynamic performance, efficiencies, and the key important parameters of the hybrid system Solar PV Thermal and heat pipe under investigation. The model is based on dynamic mass and energy equations coupled with the heat transfer coefficients, thermodynamic constants, and material properties.

This hybrid system is composed of the novel combined concept of a Photovoltaic-Thermal Solar Panel PV and a Heat Pipe. This current study is presented under different parameters, such as solar irradiance, material properties, and boundary conditions for the Solar Pv Panel, as well as the Heat Pipe filled with different Refrigerants such as water, R-134a, R-152a, R-32, R-125, R1234fz, and R-1234fy, and R-123.

As PV Solar Panel efficiency calculations showed, the higher the solar radiation, the higher the solar PV current, and consequently, this increases the Solar Pv Power Output; however, the PV solar panel efficiency remains constant at 22.38 %.

It is pretty clear from the results presented during the course of this investigation that the higher the solar radiation, the higher the evaporator temperatures and heat pipe temperature, and obviously, the higher the thermal heat transferred to the Heat Pipe evaporator section, and consequently, the higher the heat released from the heat pipe condenser section in the thermal tank. Furthermore, the data also shows that the higher the solar radiation is, the higher the water temperature in the thermal tank, which is supplied to the domestic or industrial demand.

In addition, the data presented also demonstrated that the refrigerants R-32 and R-125 yield the maximum efficiency of the Hybrid System among the other refrigerants under investigation.

Finally, the present model predicted well the Solar PV characteristics and the thermal behavior of the heat pipes, as well as the water temperature dynamic profile.

This is an open access article under the CC BY-NC-ND license (http://creativecommons.org/licenses/by-nc-nd/4.0/)

Nomenclature

$Area_{cell}$ PV cell area (m^2)
$Area_{pipe}$ Pipe area (m^2)
$Area_{HT}$ Heat transfer area (m^2)
C_{p_water} Thermal capacity of water (J/kgK)
D Internal Pipe diameter (m)
E_{gO} Bandgap energy of semiconductor (1.1 eV)
G Total Solar radiation incident on the PV module (W/m^2)
H Convective heat transfer coefficient module (W/m^2K)
h_{water} Heat transfer coefficient (W/m^2K)
Refrigerant enthalpy
I Output current of the PV module (A)
I_o Diode saturation current per module (A)
I_{ph} Light generated current per module or photocurrent (A)
I_{rs} Module reverse saturation current (A)
I_{sc} Short circuit current (A)
k Boltzmann's constant ($1.3806503*10^{-23}$J/K)
Ki Short-circuit of a PV cell at SRC (mA/°C)
K_{Pv} Thermal conductivity of Pv cell (W/mK)
L_{cell} Length of a PV cell (m)
$\dot{m}$ Water flow (Kg/s)
mC_{p_module} Thermal capacity of the PV module (9250 J/K)
m_{water} mass of water (Kg)
n Ideality factor of the diode (q)
N_p Total number of cells connected in parallel
N_{pipes} Number of pipes
N_s: Total number of cells connected in series
nTE number of Thermal Elements in a pipe
P Power generated by PV module (W)
Pa Atmospheric pressure of moist air (Pa)
pw Partial pressure of water vapor in moist air (Pa)
q electronic charge (C)
$Q_{conduction}$ Energy due to conduction (W in Electrical Process) (W/m^2 in Thermal Process)
$Q_{convection}$ Energy due to Convection (W in Electrical Process) (W/m^2 in Thermal Process)
Q_{elect} Electrical power generated (W)
Q_{in} Energy received due to Solar irradiation (W/m^2)
Q_{in_cell} Energy incident on one PV cell due to solar radiation (W/m^2)
$Q_{radiation}$ Energy due to radiation (W/m^2 in Thermal Process)
$Q_{Thermal}$ Energy from thermal process (W)
R_d Fouling factor - or unit thermal resistance of the deposit (m^2K/W)
R_s Diode series resistance per module (Ω)
R_{sh} Diode shunt resistance per module (Ω)
S_c Total surface area of PV cells in a module (m^2)
S_p Total area of the PV module (m^2)
T Operating temperature (k)
T Time (s)
T_a Ambient temperature (°C)
T_C Pv Cell Temperature (°C)
T_{db} Dry bulb temperature (°C)
T_f Fluid temperature (°C)
T_{f_in} Fluid temperature at inlet (°C)
T_{fHx} Maximum temperature at the heat exchanger (°C)
T_{fHx+1} Fluid temperature at thermal element 1 (dx) (°C)
T_m Module Back-surface temperature (°C)
T_r Nominal temperature (298.15 K)
U Thermal conductance of clean heat exchanger (W/m^2K)
Ud Thermal conductance of heat exchanger after fouling (W/m2K)
V Output voltage (V)
V_{oc} Open circuit voltage (V)
Vt Diode thermal voltage (V)
x Humidity ratio (kg_{water}/kg_{dry_air})
α_{abs} Overall absorption coefficient
η_{Hybrid} system efficiency
ηPvPV module efficiency
$\eta_{Thermal}$ Efficiency of thermal process
ρw Density of water vapor (Kg/m^3)
∂Q Convection heat transfer rate
Q Thermal heat (kj/s)
ε Emissivity of PV cells

Acknowledgement

The research work presented in this paper was made possible through the support of the Catholic University of Cuenca. The author would also like to thank Edwin Marin for his great help in performing the different computations.

References

[1] D.J. Yang et al., "Simulation and Experimental Validation of Heat Transfer in a Novel Hybrid Solar Panel," *International Journal of Heat and Mass Transfer*, vol. 55, no. 4, pp. 1076-1082, 2012. [CrossRef] [Google Scholar] [Publisher Link]

[2] Pei Gang et al., "A Numerical and Experimental Study on a Heat Pipe PV/T System," *Solar Energy*, vol. 85, no. 5, pp. 911-921, 2011. [CrossRef] [Google Scholar] [Publisher Link]

[3] Nannan Dai et al., "Simulation of Hybrid Photovoltaic Solar Assisted Loop Heat Pipe/Heat Pump System," *Applied Sciences*, vol. 7, no. 2, pp. 1-15, 2017. [CrossRef] [Google Scholar] [Publisher Link]

[4] Y. Tripanagnostopoulos et al., "Hybrid Photovoltaic/Thermal Solar Systems," *Sol Energy*, vol. 72, no. 3, pp. 217-234, 2002. [CrossRef] [Google Scholar] [Publisher Link]

[5] Trond Bergene, and Ole Martin Løvvik, "Model Calculations on a Flat-Plate Solar Heat-Collector with Integrated Solar Cells," *Solar Energy*, vol. 55, no. 6, pp. 453-462, 1995. [CrossRef] [Google Scholar] [Publisher Link]

[6] H.G. Teo, P.S. Lee, and M.N.A. Hawlader, "An Active Cooling System for Photovoltaic Modules," *Applied Energy*, vol. 90, no. 1, pp. 309-315, 2012. [CrossRef] [Google Scholar] [Publisher Link]

[7] H. Hashim, J.J. Bomphrey, and G. Min, "Model for Geometry Optimization of Thermoelectric Devices in a Hybrid PV/TE System," *Renewable Energy*, vol. 87, pp. 458-463, 2016. [CrossRef] [Google Scholar] [Publisher Link]

[8] H.P. Garge, and R.K. Agarwal, "Some Aspects of a PV/T Collector/Force Circulation Flat-Plate Solar Water Heater with Solar Cells," *Energy Conversion and Management*, vol. 36, pp. 87-99, 1995. [CrossRef] [Google Scholar] [Publisher Link]

[9] Abebe Endalew, "*Numerical Modeling and Experimental Validation of Heat Pipes Solar Collector for Water Heating*," KTH Industrial Engineering and Management, Sweden, 2011. [Google Scholar] [Publisher Link]

[10] BjØrnar Sandnes, and John Rekstad, "A Photovoltaic/Thermal (PV/T) Collector with a Polymer Absorber Plate, Experimental Study and Analytical Model," *Sol Energy*, vol. 72, no. 1, pp. 63-73, 2002. [CrossRef] [Google Scholar] [Publisher Link]

[11] Xudong Zhao, "*Investigation of a Novel Heat Pipe Collector/CHP System*," Nottingham University, England, 2003. [Google Scholar] [Publisher Link]

[12] Ruobing Liang, Jili Zhang, and Zhou, "Dynamic Simulation of Novel Solar Heating System Based On Hybrid Photovoltaic /Thermal Collectors (PVT)," *Procedia Engineering*, vol. 121, pp. 675-682, 2015. [CrossRef] [Google Scholar] [Publisher Link]

[13] S. Sami, and E. Marin, "Simulation of Solar Photovoltaic, Biomass Gas Turbine and District Heating Hybrid System," *International Journal of Sustainable Energy and Environmental Research*, vol. 6, no. 1, pp. 9-26, 2017. [CrossRef] [Google Scholar] [Publisher Link]

[14] Samuel Sami, and Jorge Rivera, "A Predictive Numerical Model for Analyzing Performance of Solar Photovoltaic, Geothermal Hybrid System for Electricity Generation and District Heating," *Science Journal Energy Engineering*, vol. 5, no. 1, pp. 13-30, 2017. [CrossRef] [Google Scholar] [Publisher Link]

[15] S. Sami, and E. Marin, "A Numerical Model for Predicting Performance of Solar Photovoltaic, Biomass and CHP Hybrid system for Electricity Generation," *International Journal of Engineering Sciences & Research Technology*, vol. 4, no. 1, pp. 1-22, 2017. [CrossRef] [Google Scholar] [Publisher Link]

[16] Clara Good et al., "Hybrid Photovoltaic-Thermal Systems in Buildings – A Review," *Energy Procedia*, vol. 70, pp. 683-690, 2015. [CrossRef] [Google Scholar] [Publisher Link]

[17] H.M. Faragali et al., "A Simulation Model for Predicting the Performance of PV/Wind- Powered Geothermal Space Heating System in Egypt," *The Online Journal on Electronics and Electrical Engineering*, vol. 2, no. 4, 2008. [Google Scholar]

[18] Yuanzhi Gao et al., "A Comprehensive Review of the Current Status, Developments, and Outlooks of Heat Pipe Photovoltaic and Photovoltaic/Thermal Systems," *Renewable Energy*, vol. 207, pp. 539-574, 2023. [CrossRef] [Google Scholar] [Publisher Link]

[19] S. Sami, and E. Marin, "Dynamic Modeling and Simulation of Hybrid Solar Photovoltaic and PEMFC Fuel Power System," *RA Journal of Applied Research*, vol. 4, no. 5, pp. 1664-1683, 2018. [CrossRef] [Google Scholar] [Publisher Link]

[20] F. Tardy, and Samuel M. Sami, "Thermal Analysis of Heat Pipes During Thermal Storage," *Applied Thermal Engineering*, vol. 29, no. 2-3, pp. 329-333, 2009. [CrossRef] [Google Scholar] [Publisher Link]

[21] John Duffie, *Solar Engineering of Thermal Processes*, Wiley, New York, 1991. [Google Scholar] [Publisher Link]

[22] J.M. Coulson et al., Richardson's Chemical Engineering, Sixth Edition, Fluid Flow, Heat Transfer and Mass Transfer, Butterworth–Heinemann Publishing, Oxford, UK, 1999.

[23] Heat Exchangers - Fouling and Reduced Heat Transfer. [Online]. Available: http://www.engineeringtoolbox.com/fouling-heat-transfer-d_1661.html

[24] David Reay, Ryan McGlen, and Peter Kew, *Heat Pipes*, 5th Edition, Butterworth-Heinemann Publisher, Oxford, UK, 2006. [Google Scholar] [Publisher Link]

[25] F. Tardy, and S.M. Sami, "An Experimental Study Determining Behaviour of Heat Pipes in Thermal Storage," *International Journal of Ambient Energy*, vol. 29, no. 3, pp. 162-168, 2008. [CrossRef] [Google Scholar] [Publisher Link]

[26] A. Sweidan, N. Ghaddara, and K. Chali, "Optimized Design and Operation of Heat-Pipe Photovoltaic Thermal System with Phase Change Material for Thermal Storage," *Journal of Renewable and Sustainable Energy*, vol. 8, no. 2, 2016. [CrossRef] [Google Scholar] [Publisher Link]

[27] S. Sami, and C. Campoverde, "Dynamic Simulation and Modeling of a Novel Combined Photovoltaic – Thermal Panel Hybrid System," *International Journal of Sustainable Energy and Environmental Research*, vol. 7, no. 1, pp. 1-23, 2018. [Google Scholar] [Publisher Link]

[28] Zhao Xuxin et al., "Comparative Study on Performances of a Heat-Pipe PV/T System and a Heat-Pipe Solar Water Heating System," *International Journal of Green Energy*, vol. 13, no. 3, pp. 229-240, 2016. [CrossRef] [Google Scholar] [Publisher Link]

[29] Mohammad Sajad Naghavi et al., "Analytical Thermal Modeling of a Heat Pipe Solar Water Heater System Integrated With Phase Change Material," *Computer Applications in Environmental Sciences and Renewable Energy*, pp. 197-208, 2015. [Google Scholar]

[30] Athula Rajapakse, and Supachart Chungpaibulpantana, "Dynamic Simulation of a Photovoltaic Refrigeration System," *RERIC International Energy Jounal*, vol. 16, no. 3, pp. 67-101, 1994. [Google Scholar]

[31] [Online]. Available: http://www.boulder.nist.gov/div838/theory/refprop/LINKING/Linking.htm#ExcelApplications

[32] Jens Glembin et al., "Thermal Storage Tanks in High Efficiency Heat Pump Systems – Optimized Installation and Operation Parameters," *Energy Procedia*, vol. 73, pp. 331-340, 2015. [CrossRef] [Google Scholar] [Publisher Link]

[33] Rahmat Iman Mainil, Faisal Afif, and Dodi Sofyan Arief, "Performance Comparison of Photovoltaic (PV), Heat Pipe Photovoltaic/Thermal (HP-PV/T), and Heat Pipe Solar Thermal Collectors (HP-STC): Energy Analysis," *International Journal of Heat and Technology*, vol. 42, no. 3, pp. 897-904, 2024. [CrossRef] [Google Scholar] [Publisher Link]

[34] Hussein A. Kazem et al., "A Systematic Review of Photovoltaic/Thermal Applications in Heat Pump Systems," *Solar Energy*, vol. 269, 2024. [CrossRef] [Google Scholar] [Publisher Link]